The Darken Relation for Multicomponent Diffusion in Liquid Mixtures of Linear Alkanes: An Investigation Using Molecular Dynamics (MD) Simulations

R. Krishna* and J. M. van Baten

Van 't Hoff Institute for Molecular Sciences, University of Amsterdam, Nieuwe Achtergracht 166, 1018 WV Amsterdam, The Netherlands

Molecular dynamics (MD) simulations have been performed for binary, ternary, and quaternary liquid mixtures of linear alkanes containing 1−16 carbons. Both the self-diffusivities ($D_{i,\text{self}}$) and the Maxwell−Stefan (M−S) diffusivities ($Đ_{ij}$) were determined from the MD simulations for various mixture compositions. The self-diffusivity was determined to be a linear function of the mass fractions ω_j of the constituent species in the mixture: $D_{i,\text{self}} = \sum_{j=1}^{j=n} \omega_j D_{i,\text{self}}^{x_j \to 1}$ where $D_{i,\text{self}}^{x_j \to 1}$ is the self-diffusivity of infinitely dilute species i in species j. The Maxwell−Stefan diffusivity of the binary $i-j$ pair in a multicomponent mixture was determined to be predicted reasonably well by the generalization of the Darken relation: $Đ_{ij} = [x_i/(x_i + x_j)]D_{j,\text{self}} + [x_j/(x_i + x_j)]D_{i,\text{self}}$, where x_i is the mole fraction of species i.

1. Introduction

Many equally rigorous descriptions of diffusive mass transport have appeared in the literature since the development of Fick's law. One of these formulations, the Maxwell−Stefan (M−S) equations,[1−6]

$$-\frac{1}{RT}\nabla\mu_i = \sum_{j=1;j\neq i}^{j=n} \frac{x_j(\mathbf{u}_i - \mathbf{u}_j)}{Đ_{ij}} \qquad (\text{for } i,j = 1, 2, ..., n) \tag{1}$$

provides the most convenient, and practical, description of diffusion in n-component fluid mixtures. In eq 1, $\mathbf{u}_i$ is the ensemble-averaged velocity of species i, $\mathbf{u}_i = \langle \mathbf{v}_i \rangle$, x_i is the mole fraction of species i, and $Đ_{ij}$ is the M−S diffusivity of the $i-j$ pair in the mixture. The chemical potential gradients satisfy the Gibbs−Duhem relationship,

$$\sum_{i=1}^{n} x_i \nabla\mu_i = 0 \tag{2}$$

and, therefore, only $n - 1$ of the driving forces in eq 2 are independent. If $\mathbf{u}$ represents the molar average reference velocity,

$$\sum_{i=1}^{n} x_i \mathbf{u}_i = \mathbf{u} \tag{3}$$

we can cast eq 1 into $(n - 1)$-dimensional matrix form:

$$-\frac{x_i}{RT}\nabla\mu_i = \sum_{j=1}^{n-1} B_{ij} x_j (\mathbf{u}_j - \mathbf{u}) \qquad (\text{for } i = 1, 2, ..., n-1) \tag{4}$$

where we may define an $(n - 1)$-dimensional matrix $[B]$ as

$$B_{ii} = \frac{x_i}{Đ_{in}} + \sum_{j=1;j\neq i}^{n} \frac{x_j}{Đ_{ij}} \tag{5a}$$

and

$$B_{ij,j\neq i} = -x_i\left(\frac{1}{Đ_{ij}} - \frac{1}{Đ_{in}}\right) \qquad (\text{for } i,j = 1, 2, ..., n-1) \tag{5b}$$

The M−S diffusivities $Đ_{ij}$ are independent of the reference frame, and the Onsager reciprocal relations imply the symmetry property:[1]

$$Đ_{ij} = Đ_{ji} \tag{6}$$

For ideal gas mixtures, the $Đ_{ij}$ values are independent of the mixture composition. However, for liquid mixtures the $Đ_{ij}$ values are dependent on composition.[2,3,7]

Let us define the diffusion fluxes $\mathbf{J}_i$, with respect to the molar average reference velocity $\mathbf{u}$:

$$\mathbf{J}_i = c_i(\mathbf{u}_i - \mathbf{u}) \equiv c x_i(\mathbf{u}_i - \mathbf{u}) \qquad (\text{for } i = 1, 2, ..., n) \tag{7}$$

For a binary mixture, the Fick diffusivity (D_{12}) is defined by

$$\mathbf{J}_1 = -cD_{12}\nabla x_1 = -\mathbf{J}_2 = cD_{12}\nabla x_2 \tag{8}$$

and is equal to the M−S diffusivity multiplied by the thermodynamic correction factor Γ:

$$D_{12} \equiv Đ_{12}\Gamma = Đ_{12}\left(\frac{\partial \ln a_1}{\partial \ln x_1}\right) \tag{9}$$

where a_1 is the activity of component 1 ($a_1 = \gamma_1 x_1$).

The Darken relation[8] postulates that the composition dependence of the Fick diffusivity D_{12} is given by

$$D_{12} = (x_2 D_{1,\text{self}} + x_1 D_{2,\text{self}})\left(\frac{\partial \ln a_1}{\partial \ln x_1}\right) \tag{10}$$

where $D_{1,\text{self}}$ and $D_{2,\text{self}}$ are tracer diffusivities (or self-

* To whom correspondence should be addressed. Fax: +31 20 5255604. E-mail: r.krishna@uva.nl.

10.1021/ie050146c CCC: $30.25
Published on Web 07/07/2005

diffusivities) of components 1 and 2, respectively, in the mixture. Combining eqs 9 and 10, we obtain the following expression for the composition dependence of the M−S diffusivity $Đ_{12}$ in a *binary* mixture:

$$Đ_{12} = x_2 D_{1,\text{self}} + x_1 D_{2,\text{self}} \tag{11}$$

$D_{1,\text{self}}$ and $D_{2,\text{self}}$ are more easily accessible, both experimentally[9−11] and from MD simulations,[5,6,12−23] than $Đ_{12}$. The self-diffusivities are themselves composition-dependent and lie between their respective infinite dilution limits:

$$D_{1,\text{self}}^{x_2\to 1} < D_{1,\text{self}} < D_{1,\text{self}}^{x_1\to 1} \tag{12a}$$

$$D_{2,\text{self}}^{x_2\to 1} < D_{2,\text{self}} < D_{2,\text{self}}^{x_1\to 1} \tag{12b}$$

where we use the convention that species 1 is more mobile than species 2. The four infinite dilution self-diffusivities for a binary mixture $D_{i,\text{self}}^{x_j\to 1}$ can be estimated, using the many empirical and semiempirical correlations available in the literature.[2,24−29]

An alternative to the Darken relation is the logarithmic interpolation formula that was devised by Vignes:[30]

$$Đ_{12} = (Đ_{12}^{x_1\to 1})^{x_1}(Đ_{12}^{x_2\to 1})^{x_2} \equiv (D_{2,\text{self}}^{x_1\to 1})^{x_1}(D_{1,\text{self}}^{x_2\to 1})^{x_2} \tag{13}$$

Other interpolation formulas have also been suggested in the literature.[25,27,31]

The description of the composition dependence of the M−S diffusivities $Đ_{ij}$ in liquid mixtures containing three or more species is much less developed. For a ternary mixture, Wesselingh and Bollen[32] have suggested the following extension of the Vignes relationship:

$$Đ_{ij} = (Đ_{ij}^{x_i\to 1})^{x_i}(Đ_{ij}^{x_j\to 1})^{x_j}(Đ_{ij}^{x_k\to 1})^{x_k} \tag{14}$$

The estimation of the $Đ_{ij}^{x_k\to 1}$, which is the $i-j$ pair diffusivity when both i and j are present in infinitely dilute concentrations, is particularly uncertain, and Wesselingh and Bollen[32] have tentatively suggested

$$Đ_{ij}^{x_k\to 1} = \sqrt{Đ_{ik}^{x_k\to 1}\, Đ_{jk}^{x_k\to 1}} \tag{15}$$

for "lack of better". Kooijman and Taylor[33] have presented some calculations to suggest that eqs 14 and 15 provide reasonably good agreement with experimental data. As yet, no fundamental justification to eq 15 has been presented.

The major objective of the present communication is to investigate the composition dependence of the self-diffusivities $D_{\text{i,self}}$ and the M−S diffusivities $Đ_{ij}$ in binary, ternary, and quaternary liquid mixtures of linear alkanes using molecular dynamics (MD) simulations. We develop the proper generalization of the Darken relation for multicomponent mixtures. Furthermore, we provide a fundamental basis for the estimation of $Đ_{ij}^{x_k\to 1}$.

2. Molecular Dynamics Simulations

The details of the MD simulation technique used to determine the self-diffusivity and M−S diffusivity in pure-component and binary mixtures are well-documented in the literature,[5,6,12−23] and we highlight only the major issues relevant to n-alkane mixtures; the code used was essentially identical to that used to investigate diffusion of n-alkane mixtures in zeolites.[34,35] We use the united atom model and consider the CH_x groups as single, chargeless interaction centers with their own effective potentials. The beads in the chain are connected by harmonic bonding potentials. A harmonic cosine bending potential models the bond bending between three neighboring beads, and a Ryckaert−Bellemans potential controls the torsion angle. The beads in a chain separated by more than three bonds interact with each other through a Lennard-Jones potential. The Lennard-Jones potentials are shifted and cut at 12 Å. The force fields have been given in detail in other publications.[36,37] The size of the simulation box was taken to be either 25 Å × 25 Å × 25 Å or 30 Å × 30 Å × 30 Å; the larger box was used for mixtures that contained nC6, nC12, and nC16 alkanes. Periodic boundary conditions were used.

Diffusion in a system of N molecules is simulated using Newton's equations of motion until the system properties, on average, no longer change with time. The Verlet algorithm is used for time integration. The energy drift of the entire system is monitored to ensure that the time steps taken were not too large. A time step of 2 fs was used in all simulations. N molecules are inserted into the simulation box at random positions as long as no overlaps occur with other particles. During the initializing period, we perform an NVT MC simulation to rapidly achieve an equilibrium molecular arrangement. After the initialization step, we assign velocities to the pseudo-atoms from the Maxwell−Boltzmann distribution at the desired average temperature. The total momentum of the system is set to zero. Next, we equilibrate the system further by performing a NVT MD simulation using the Nosé−Hoover thermostat. When the equilibration is completed, the production run starts. For every cycle, the statistics for determining the mean square displacements (MSDs) in the NVT ensemble are updated. The MSDs are determined for time intervals ranging from 2 fs to 1 ns. To do this, an order-N algorithm, as detailed in Chapter 4 of Frenkel and Smit,[23] is implemented.

The self-diffusivities were determined from the formula

$$D_{i,\text{self}} = \frac{1}{6N_i}\lim_{\Delta t\to\infty}\frac{1}{\Delta t}\left\langle\left(\sum_{l=1}^{N_i}(\mathbf{r}_{l,i}(t+\Delta t) - \mathbf{r}_{l,i}(t))^2\right)\right\rangle \tag{16}$$

where $\mathbf{r}_{l,i}(t)$ denotes the position vector of molecule l of species i, N_i is the number of molecules of species i, and the notation $\langle\cdots\rangle$ denotes ensemble averaging. The elements of the n-dimensional matrix of Onsager coefficients [Λ], which are defined by

$$x_i\mathbf{u}_i = -\frac{1}{RT}\sum_{j=1}^{n}\Lambda_{ij}\nabla\mu_j \qquad (i = 1, 2, ..., n) \tag{17}$$

are determined from

$$\Lambda_{ij} = -\frac{1}{6}\lim_{\Delta t\to\infty}\frac{1}{N}\frac{1}{\Delta t}\left\langle\left(\sum_{l=1}^{N_i}(\mathbf{r}_{l,i}(t+\Delta t) - \mathbf{r}_{l,i}(t))\right)\cdot\left(\sum_{k=1}^{N_j}(\mathbf{r}_{k,j}(t+\Delta t) - \mathbf{r}_{k,j}(t))\right)\right\rangle \tag{18}$$

where N_i and N_j are the number of molecules of species

Table 1. Simulation Campaigns

Conditions		
temperature (K)	pressure (MPa)	linear alkane mixture
333	30	binaries: C1−C2, C1−C3, C2−C3; varying mole fraction x_i in each case
333	30	ternary: C1−C2−C3; three campaigns, varying x_i, keeping $x_j/x_k = 1$
333	30	binaries: C2−C3, C2−*n*C4, C3−*n*C4; varying mole fraction x_i in each case
333	30	ternary: C2−C3−*n*C4; three campaigns, varying x_i, keeping $x_j/x_k = 1$
333	30	binaries: C3−*n*C4, C3−*n*C5, *n*C4−*n*C5; varying mole fraction x_i in each case
333	30	ternary: C3−*n*C4−*n*C5; three campaigns, varying x_i, keeping $x_j/x_k = 1$
333	30	binaries: C1−C3, C1−*n*C6, C3−*n*C6; varying mole fraction x_i in each case
333	30	ternary: C1−C3−*n*C6; three campaigns, varying x_i, keeping $x_j/x_k = 1$
333	30	binaries: C1−C2, C1−*n*C6, C2−*n*C6; varying mole fraction x_i in each case
333	30	ternary: C1−C2−*n*C6; three campaigns, varying x_i, keeping $x_j/x_k = 1$
333	30	binaries: C1−*n*C8, C1−*n*C10; varying mole fraction x_i in each case
333	30	binaries: C2−*n*C8, C2−*n*C10; varying mole fraction x_i in each case
333	30	quaternary: C1−C2−C3−*n*C4; four campaigns, varying x_i, keeping $x_j/x_k = 1$; $x_k/x_l = 1$
308		binaries: *n*C6−*n*C12, *n*C6−*n*C16, *n*C12−*n*C16; varying mole fraction x_i in each case
308		ternary: *n*C6−*n*C12−*n*C16; three campaigns, varying x_i, keeping $x_j/x_k = 1$

i and j, respectively, in the simulations box and N represents the total number of molecules. The Onsager coefficients defined by eq 17 correspond to a reference frame in which the mass-average mixture velocity is zero, i.e., $\sum_{i=1}^{n} \omega_i \mathbf{u}_i = 0$. This implies that the Onsager coefficients are constrained by

$$\sum_i M_i \Lambda_{ij} = 0 \tag{19}$$

where M_i represents the molar mass of species i. We verified that eq 19 was satisfied in all our simulations. Furthermore, the Onsager reciprocal relations require that $\Lambda_{ij} = \Lambda_{ji}$.

Let us define an $(n - 1)$-dimensional matrix $[\Delta]$:

$$[\Delta] = [B]^{-1} \tag{20}$$

where the matrix $[B]$ is given by eq 5. The elements Δ_{ij} are related to the Onsager coefficients Λ_{ij} by

$$\Delta_{ij} = (1 - x_i)\left(\frac{\Lambda_{ij}}{x_j} - \frac{\Lambda_{in}}{x_n}\right) - x_i \sum_{k=1;k\neq i}^{k=n}\left(\frac{\Lambda_{kj}}{x_j} - \frac{\Lambda_{kn}}{x_n}\right) \quad (i, j = 1, 2, ..., n - 1) \tag{21}$$

For a binary mixture, $n = 2$, the matrix $[\Delta]$ degenerates to a scalar quantity Δ_{11} that is identical to the M−S diffusivity $Đ_{12}$:

$$Đ_{12} \equiv \Delta_{11} = x_2\left(\frac{\Lambda_{11}}{x_1} - \frac{\Lambda_{12}}{x_2}\right) - x_1\left(\frac{\Lambda_{21}}{x_1} - \frac{\Lambda_{22}}{x_2}\right) = \frac{x_2}{x_1}\Lambda_{11} + \frac{x_1}{x_2}\Lambda_{22} - \Lambda_{12} - \Lambda_{21} \tag{22}$$

An alternative derivation of eq 22 is given by Van de Ven-Lucassen et al.[22] For mixtures of three or more components, the M−S diffusivities $Đ_{ij}$ can be calculated by combining eqs 5, 20, and 21. The detailed derivation of eq 21, along with the relations for calculation of the $Đ_{ij}$, are available in Appendix B of the Supporting Information associated with this publication.

We performed MD simulations to determine the self-diffusivities $D_{i,\text{self}}$ and the M−S diffusivities $Đ_{ij}$ in binary, ternary, and quaternary mixtures that contained methane (C1), ethane (C2), propane (C3), *n*-butane (*n*C4), *n*-pentane (*n*C5), and/or *n*-hexane (*n*C6) at a temperature of 333 K and a total pressure of 30 MPa. The simulation campaigns are specified in Table 1. The binary mixtures were investigated over the entire composition range to the pure-component limits. For the ternary mixtures, three types of campaigns were undertaken. In each campaign, the mole fraction of one of the components (x_i) was varied while maintaining equimolar proportions of the remaining two species, i.e., $x_j/x_k = 1$. For the simulations with the quaternary mixture of C1−C2−C3−*n*C4, four types of campaigns were undertaken. In each campaign, the mole fraction of one of the components (x_i) was varied while maintaining equimolar proportions of the remaining three species (i.e., $x_j/x_k = x_k/x_l = 1$). For every campaign, the mixture density was estimated for each mixture, using the Peng−Robinson equation of state.[24] This estimated mixture density was used to determine the number of molecules of the individual species to be used within the simulation box. Table 2 gives an example of the molecular loadings in the 25 Å × 25 Å × 25 Å simulation box for the binary mixture of C1 and C3. We also conducted a few μPT CBMC simulations, to calculate the molecular loadings in the simulation box; the deviations from those estimated from the Peng−Robinson equation of state were observed to be <7%.

Table 2. Details of Number of Molecules in the 25 Å × 25 Å × 25 Å Simulation Box for Binary Mixtures of Methane (C1) and Propane (C3) at 333 K and 30 MPa

Number of Molecules		mixture	mole	mass
C1 (1)	C3 (2)	density, ρ	fraction, x_i	fraction, ω_i
0	117	548.3	0.0000	0.0000
6	112	535.1	0.0508	0.0191
12	108	526.6	0.1000	0.0389
18	103	513.4	0.1488	0.0598
24	97	495.5	0.1983	0.0826
31	92	484.0	0.2520	0.1092
37	87	470.8	0.2984	0.1340
44	81	454.6	0.3520	0.1650
50	75	436.7	0.4000	0.1952
56	69	418.8	0.4480	0.2280
63	63	402.7	0.5000	0.2668
69	56	380.1	0.5520	0.3095
75	50	362.2	0.6000	0.3531
80	43	337.9	0.6504	0.4036
85	37	318.3	0.6967	0.4553
90	30	294.0	0.7500	0.5219
95	24	274.5	0.7983	0.5902
99	17	248.5	0.8534	0.6794
103	11	227.2	0.9035	0.7731
106	6	208.8	0.9464	0.8654
110	0	187.6	1.0000	1.0000

In addition, we performed MD simulations for binary and ternary mixtures that contained *n*C6, *n*C12, and *n*C12 at a temperature of 308 K (see Table 1). In this case, the mixture density was estimated from the

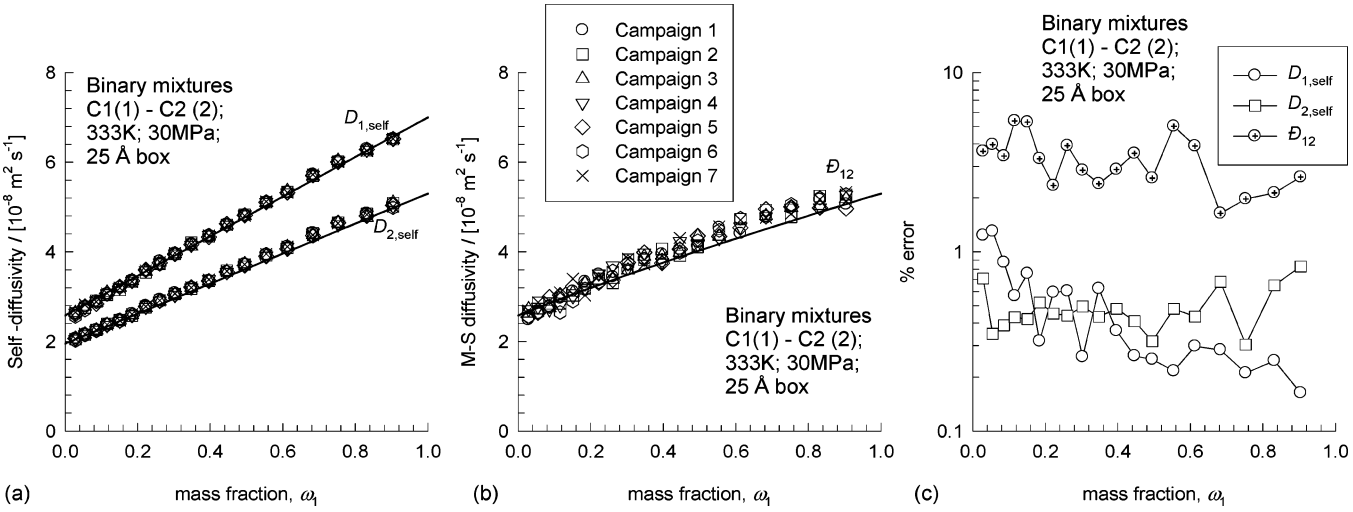

Figure 1. Molecular dynamics (MD) simulation results for seven different campaigns to determine (a) self-diffusivities ($D_{i,self}$) and (b) M−S diffusivities ($Đ_{12}$) in a binary C1−C2 mixture at 333 K and 30 MPa, as a function of mass fraction in the mixture. (c) Estimate of errors in the determination of $D_{i,self}$ and $Đ_{12}$. The straight lines in Figure 1a have been drawn using eq 23 with the parameters specified in Table 3. The continuous line in Figure 1b is drawn using the Darken relation (eq 11). The simulation box size used was 25 Å × 25 Å × 25 Å.

experimental data available in the literature,[9,10] and this information was used to determine the molecular loadings in the simulation box.

The complete set of data on $D_{i,self}$ and $Đ_{ij}$ for each campaign has been presented separately, in graphical form, in Appendix A of the Supporting Information associated with this publication, which also contains the molecular loadings used in the simulation box for each individual campaign. Below, we present a representative selection of the results with the objective of drawing general conclusions.

The bulk of the simulations were conducted on clusters of personal computers (PCs) that were equipped with Intel Xeon processors running at 3.4 GHz on the Linux operating system. Each simulation campaign run was run for a period long enough to obtain reliable statistics for determination of the diffusivities (ranging from a minimum of 24 h to a maximum of 168 h). The required simulation time increases both with the number of molecules in the simulation box and the chain length of the molecules in the mixture.

3. Simulation Results and Discussion

Let us first address the issue of accuracy and reproducibility of the MD simulation results. In Figure 1a and b, we present the results obtained in a 25 Å × 25 Å × 25 Å box, from seven different simulation campaigns, for self-diffusivities $D_{i,self}$ (Figure 1a) and M−S diffusivities $Đ_{12}$ (Figure 1b) in binary C1−C2 mixtures of varying composition. The errors in the determination of $D_{i,self}$ and $Đ_{12}$ are shown in Figure 1c; these errors are defined as the standard deviations, as percentages of the average values. The self-diffusivities $D_{i,self}$ are accurate to within 1%; the M−S diffusivities $Đ_{12}$ are accurate to within 5%. The diffusivity values are considered to be sufficiently accurate to achieve the objectives that have been determined in this paper. The simulation results for other mixtures presented in this paper are for one simulation campaign, each, for a specified mixture composition.

For the binary C1−*n*C6 mixture, the results of simulations with boxes with sizes of 25 Å × 25 Å × 25 Å and 30 Å × 30 Å × 30 Å are compared in Figure 2a. Both box sizes yield comparable results. Note that the simulation with the larger box requires a longer simulation time. For all mixtures containing alkanes with 1−6 carbons, a simulation box 25 Å × 25 Å × 25 Å in size was determined to yield results of acceptable accuracy. For mixtures that contained *n*C6, *n*C12, and *n*C16 alkanes, a simulation box 30 Å × 30 Å × 30 Å in size was used.

Let us consider the self-diffusivities in unary systems, $D_{i,self}^{x_i\to 1}$, for alkanes of 1−10 carbons at a temperature of 333 K and a pressure of 30 MPa. The MD simulated results are compared with the experimental data of Helbaek et al.[11] in Figure 3a. The agreement of the MD simulations with experimental data is good for the entire range of carbon numbers, providing evidence of the accuracy of our simulations and also of the force fields used. In Figure 3b and c, the self-diffusivities $D_{i,self}$ in binary mixtures of C1−*n*C6 and C1−*n*C8 are observed to be in very good agreement with the experimental data of Helbaek et al.[11] Both MD simulation results and experimental data show that the self-diffusivities of each individual species in the binary mixtures are linear functions of the *mass* fractions, ω_i:

$$D_{1,self} = \omega_1 D_{1,self}^{x_1\to 1} + \omega_2 D_{1,self}^{x_2\to 1}$$
$$D_{2,self} = \omega_1 D_{2,self}^{x_1\to 1} + \omega_2 D_{2,self}^{x_2\to 1} \qquad (23)$$

For comparison, the variation of the self-diffusivities with mole fractions (x_1) and volume fractions (ϕ_1) in the mixture are shown in Figure 2b and c, respectively, for the binary C1−*n*C6 mixture. The self-diffusivities are clearly *not* linearly dependent on the mole fractions. The logarithmic of the self-diffusivities are observed to be linearly dependent on the volume fraction ϕ_1, i.e.,

$$D_{1,self} = (D_{1,self}^{x_1\to 1})^{\phi_1}(D_{1,self}^{x_2\to 1})^{\phi_2}$$
$$D_{2,self} = (D_{2,self}^{x_1\to 1})^{\phi_1}(D_{2,self}^{x_2\to 1})^{\phi_2} \qquad (24)$$

The basis of the composition dependence expressed in eq 24 lies in the free volume theory of liquid diffusion.[7]

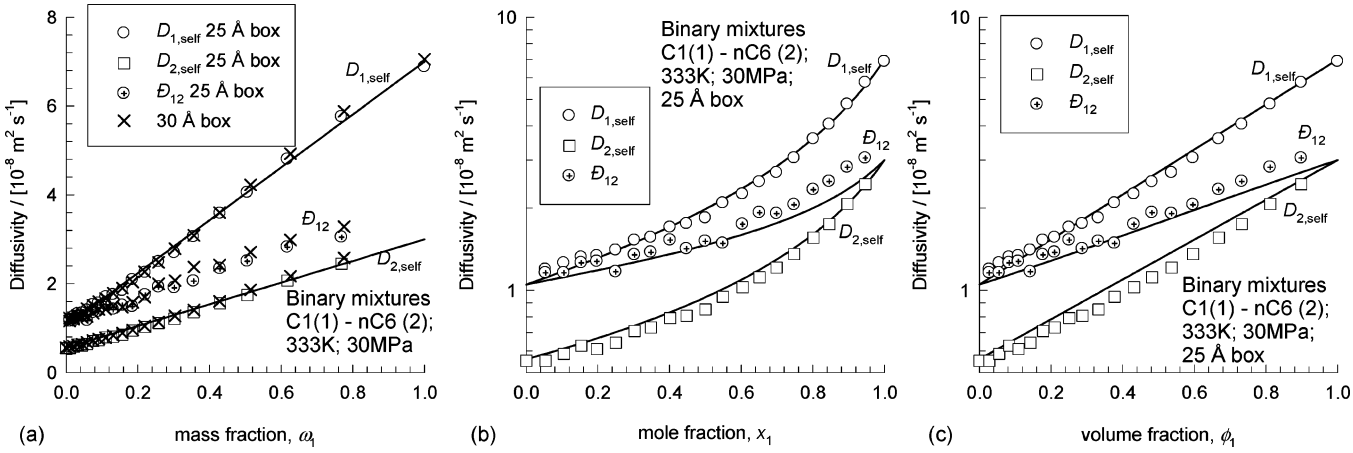

Figure 2. (a) Comparison of MD simulation results for self-diffusivity $D_{i,\text{self}}$, and M−S diffusivity Đ$_{12}$, as a function of the mass fraction ω_1 in binary C1−nC6 mixture at 333 K and 30 MPa obtained with two different simulation box sizes of 25 Å × 25 Å × 25 Å and 30 Å × 30 Å × 30 Å. (b) Simulation results for $D_{i,\text{self}}$ and Đ$_{12}$ in a binary C1−nC6 mixture obtained with a 25 Å × 25 Å × 25 Å box, plotted as a function of the mole fraction x_1. (c) Simulation results for $D_{i,\text{self}}$, and diffusivities Đ$_{12}$ in a binary C1−nC6 mixture obtained with a 25 Å × 25 Å × 25 Å box, plotted as a function of volume fraction ω_1.

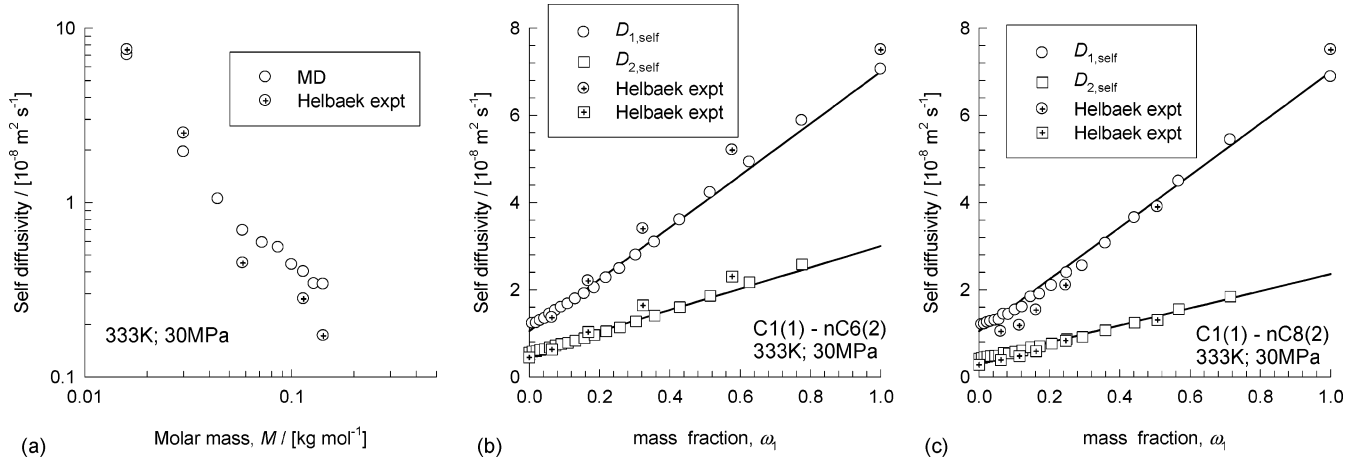

Figure 3. Self-diffusivities in (a) pure alkanes of 1−10 carbons, (b) binary mixtures of C1−nC6, and (c) binary mixtures of C1−nC8 at 333 K and 30 MPa. The MD simulation results (open symbols) are compared with the experimental data of Helbaek et al.[11] (denoted by symbols containing crosses). The straight lines in Figure 3b and Figure 3c have been drawn using eq 23 with the parameters specified in Table 3.

The linear dependence of the self-diffusivities $D_{i,\text{self}}$ on the mass fractions can also been observed in the MD simulation results for diffusion of linear alkane mixtures reported by Harmandaris et al.[19] For long alkanes, the chain-end free-volume theory proposed by Buesche[38] and von Meerwall and co-workers[39,40] provides some theoretical background for this observed linear dependence of $D_{i,\text{self}}$ on the mass fractions. This linear dependence was observed for every binary mixture investigated in this work; this can be verified by examining the graphs for all binary mixtures that have been presented in Appendix A in the Supporting Information associated with this publication. The infinite dilution self-diffusivities $D_{i,\text{self}}^{x_j\to 1}$, obtained from the unary and binary mixture data, have been presented in Tables 3 and 4.

Equation 23 would suggest the following generalization of the composition dependence of $D_{i,\text{self}}$ to n-component mixtures:

$$D_{i,\text{self}} = \sum_{j=1}^{j=n} \omega_j D_{i,\text{self}}^{x_j\to 1} \tag{25}$$

This generalization was determined to be valid for all ternary mixture campaigns performed in this study; an example is presented in Figure 4a−c for the three campaigns with the ternary mixture C1−C2−C3, varying the composition of each species in turn. The straight lines have been drawn using eq 25 with the parameters specified in Table 3. When we consider that the parameters $D_{i,\text{self}}^{x_j\to 1}$ have been obtained only from unary and binary mixture data, the agreement of eq 25 with the MD simulated $D_{i,\text{self}}$ must be regarded as very good.

Table 3. Self-diffusivities $D_{i,self}^{x_j\to 1}$ for Linear Alkanes at 333 K and 30 MPa[a]

	Self-diffusivity, $D_{i,\text{self}}^{x_j\to 1}$ (× 10^{-8} m^2/s)									
	C1	C2	C3	nC4	nC5	nC6	nC7	nC8	nC9	nC10
C1	7.00	2.58	1.50	1.05		1.05		1.05		1.05
C2	5.30	1.95	1.23	0.92		0.84		0.83		0.83
C3	4.52	1.63	1.03	0.79	0.72	0.75				
nC4	3.83	1.44	0.92	0.69	0.65					
nC5			0.83	0.62	0.59					
nC6	3.00	1.09	0.77			0.56				
nC7							0.44			
nC8	2.36	0.97						0.40		
nC9									0.34	
nC10	1.86	0.82								0.34

[a] The rows indicate species i and the columns indicate species j.

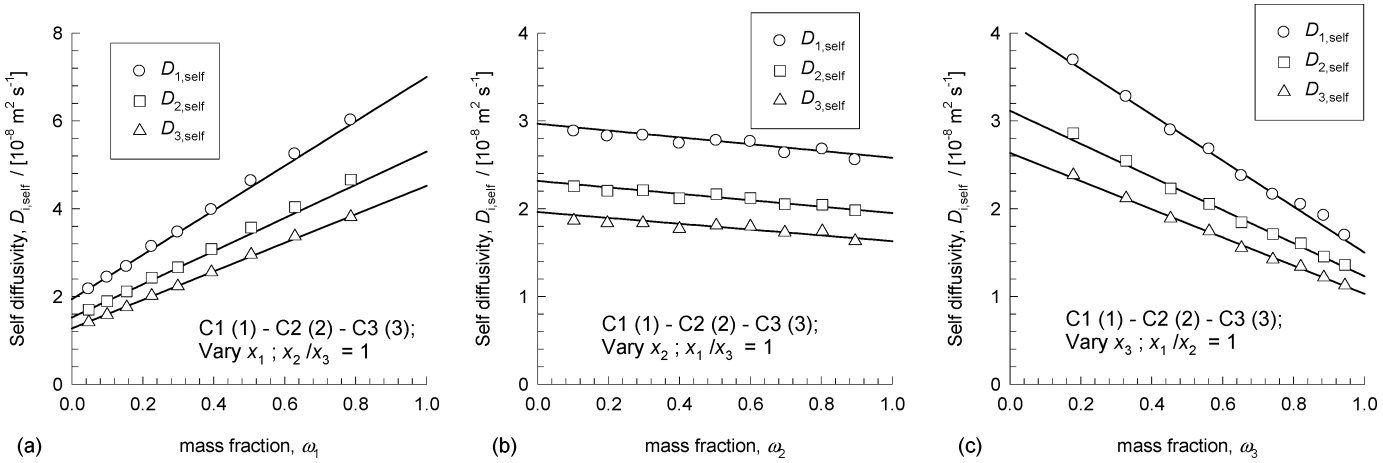

Figure 4. Self-diffusivities in the ternary mixture C1−C2−C3 with varying compositions of (a) C1, (b) C2, and (c) C3. The straight lines have been drawn using eq 25 with the parameters specified in Table 3.

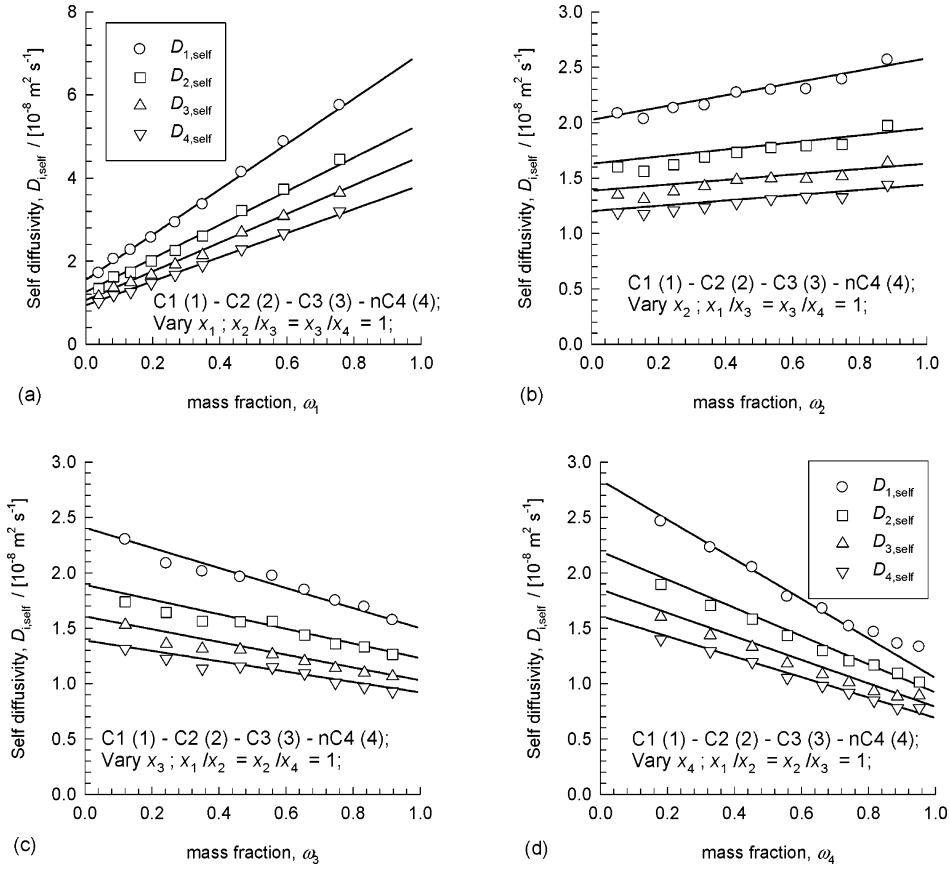

Figure 5. Self-diffusivities in the quaternary mixture C1−C2−C3−*n*C4 with varying compositions of (a) C1, (b) C2, (c) C3, and (d) *n*C4. The straight lines have been drawn using eq 25 with the parameters specified in Table 3.

Similar good agreement between the calculations following eq 25 with MD simulations have been obtained for *all* ternary mixtures studied. This good agreement also extends to four campaigns with the quaternary mixture C1−C2−C3−*n*C4, as is evidenced in Figure 5a−d.

Now let us turn to the composition dependence of the M−S diffusivities Đ$_{12}$. Consider the binary mixtures C1 with C2, C3, *n*C4, and *n*C6. The MD simulated values (open symbols) are compared with the predictions following the Darken relation (eq 11) (continuous solid lines) in Figure 6a. In these predictions, the self-diffusivities are calculated using eq 25 with the parameters specified in Table 3. The agreement of the Darken relation with the MD simulated values are good for all systems over the entire range of compositions. Similar good agreement is obtained for binary mixtures containing C2 (Figure 6b), C3 (Figure 6c), and *n*C6 (Figure 6d). The Vignes relation[30] suggests that the logarithm of the

Table 4. Self-diffusivities $D_{i,\mathrm{self}}^{x_j\to 1}$ for Liquid Mixtures of *n*C6, *n*C12, and *n*C16 at 308 K[a]

	Self-diffusivity, $D_{i,\mathrm{self}}^{x_j\to 1}$ (× 10^{-8} m^2/s)		
	*n*C6	*n*C12	*n*C16
*n*C6	0.570	0.216	0.150
*n*C12	0.350	0.126	0.081
*n*C16	0.250	0.092	0.057

[a] The rows indicate species *i* and the columns indicate species *j*.

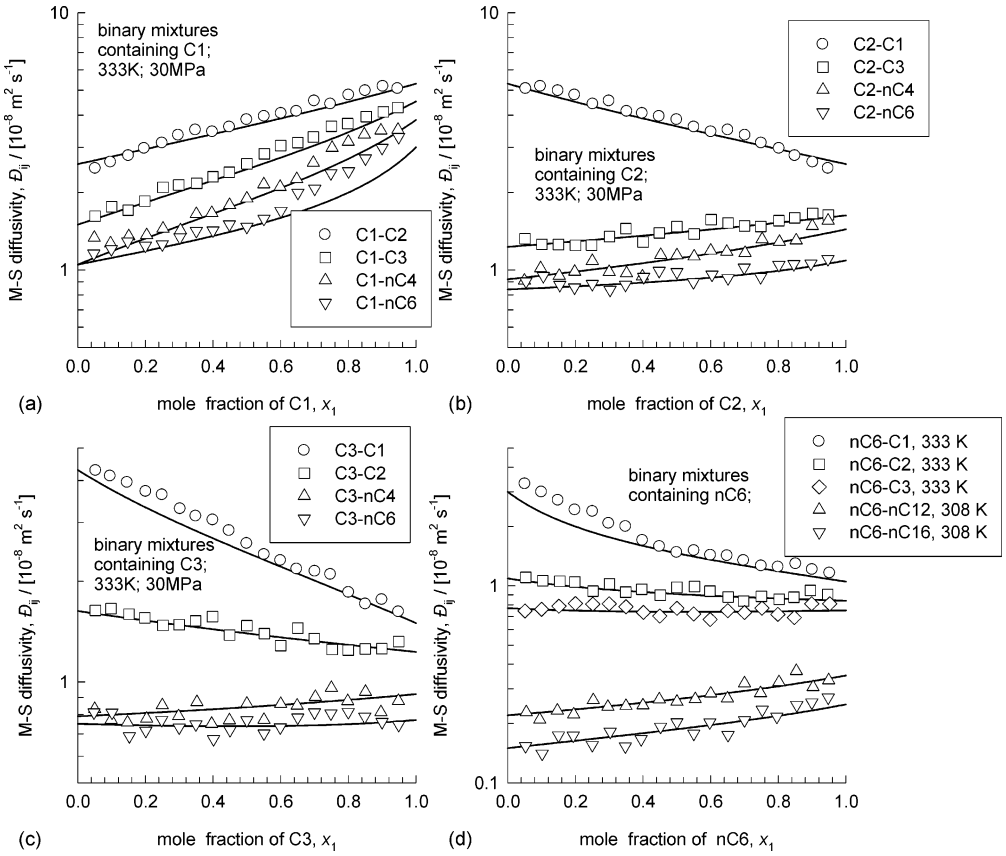

Figure 6. MD simulated values (open symbols) of the M−S diffusivity $Đ_{ij}$ for binary mixtures of (a) C1−C2, C1−C3, C1−*n*C4, and C1−*n*C6; (b) C2−C1, C2−C3, C2−*n*C4, and C2−*n*C6; (c) C3−C1, C3−C2, C3−*n*C4, and C3−*n*C6; and (d) *n*C6−C1, *n*C6−C2, *n*C6−C3, *n*C6−*n*C12, and *n*C6−*n*C16. The continuous solid lines are the calculations following the Darken relation (eq 11), where the self-diffusivities are calculated using eq 25 with the parameters specified in Tables 3 and 4. The simulations for the *n*C6−*n*C12 and *n*C6−*n*C16 binary mixtures are determined at 308 K, whereas the remaining ones are determined at 333 K and 30 MPa.

M−S diffusivity $Đ_{12}$ should be linear in the mole fraction x_1. For the C1−*n*C6 binary mixture, the Vignes relation is not valid and the Darken relation provides a better prediction of the composition dependence. Appendix A in the Supporting Information presents data for all the binary mixtures simulated, and, in all cases, good agreement is obtained between the MD-simulated $Đ_{ij}$ and the Darken relation (eq 11).

Having established the Darken relation for binary mixtures of alkanes, let us turn to ternary mixtures. Let us postulate that the M−S diffusivity of the $i-j$ pair in the ternary $i-j-k$ mixture is dependent on $D_{i,\text{self}}$ and $D_{j,\text{self}}$ in this mixture, but weighted with mole fractions on a k-free basis, i.e.,

$$Đ_{ij} = \frac{x_i}{x_i + x_j} D_{j,\text{self}} + \frac{x_j}{x_i + x_j} D_{i,\text{self}} \tag{26}$$

Because the self-diffusivity $D_{i,\text{self}}$ is dependent on all three infinite dilution values $D_{i,\text{self}}^{x_j \to 1}$, following eq 25, each of the M−S diffusivity $Đ_{ij}$ is dependent on six infinite dilution parameters. The limiting values of $Đ_{ij}$ at the edges of the ternary composition space are

$$Đ_{12}^{x_1 \to 1} = D_{2,\text{self}}^{x_1 \to 1} \tag{27a}$$

$$Đ_{12}^{x_2 \to 1} = D_{1,\text{self}}^{x_2 \to 1} \tag{27b}$$

$$Đ_{12}^{x_3 \to 1} = \frac{x_1}{x_1 + x_2} D_{2,\text{self}}^{x_3 \to 1} + \frac{x_2}{x_1 + x_2} D_{2,\text{self}}^{x_3 \to 1} \tag{27c}$$

Noting that the following limiting values hold,

$$D_{2,\text{self}}^{x_3 \to 1} = Đ_{23}^{x_3 \to 1} \tag{28a}$$

$$D_{1,\text{self}}^{x_3 \to 1} = Đ_{13}^{x_3 \to 1} \tag{28b}$$

we derive

$$Đ_{12}^{x_3 \to 1} = \frac{x_1}{x_1 + x_2} Đ_{23}^{x_3 \to 1} + \frac{x_2}{x_1 + x_2} Đ_{13}^{x_3 \to 1} \tag{29}$$

Equation 29 is the proper estimation procedure for $Đ_{12}^{x_3 \to 1}$ that is consistent with the Darken relation. If we adopt the Vignes interpolation scheme (eq 13), we obtain

$$Đ_{12}^{x_3 \to 1} = (Đ_{13}^{x_3 \to 1})^{x_1/(x_1 + x_2)} (Đ_{23}^{x_3 \to 1})^{x_2/(x_1 + x_2)} \tag{30}$$

and so we recover the Wesselingh's equation (eq 15) when species 1 and 2 are present in *equimolar* proportions but species 3 is infinitely dilute.

We demonstrate the validity of the generalized Darken relation (eq 26) by considering the ternary mixture C1−C2−C3, where the three compositions are varied, in turn, in three separate campaigns (see Figure 7a−c). The MD simulated $Đ_{ij}$ (symbols) are in reasonably good agreement with the calculations following eq 26, where the parameter values used are specified in Table 3, derived only from binary self-diffusivity data. Similar good agreement is obtained for all the ternary mixture campaigns and also the quaternary campaign, as listed

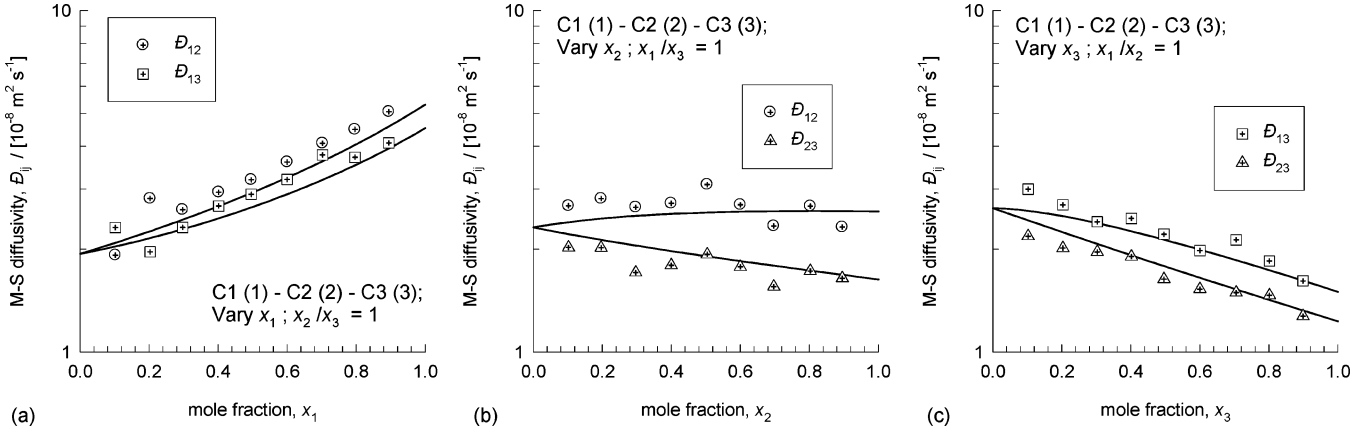

Figure 7. MD simulated values (open symbols) of the M−S diffusivity $Đ_{ij}$ for ternary mixtures of C1−C2−C3, with varying (a) x_1, (b) x_2, and (c) x_3. The continuous solid lines are the calculations following the generalized Darken relation (eq 26), where the self-diffusivities are calculated using eq 25 with the parameters specified in Table 3.

in Table 1 (see Appendix A in the Supporting Information for graphical evidence).

4. Conclusions

Using an extensive database of molecular dynamics (MD) simulations for binary mixtures containing alkanes with 1−16 carbons, we have verified the applicability of the Darken relation (eq 11) for estimation of the M−S diffusivity ($Đ_{ij}$) on the basis of information on the composition dependence of the self-diffusivities of components i and j in the binary mixture ($D_{i,\mathrm{self}}$ and $D_{j,\mathrm{self}}$, respectively). The self-diffusivity of any species is determined to be a linear function of the mass fraction in the mixture, and eq 25 provides a convenient procedure for estimation of the self-diffusivities from information on the infinite dilution values $D_{i,\mathrm{self}}^{x_j \to 1}$. The appropriate generalization of the Darken relation for the estimation of $Đ_{ij}$ in the presence of other species k is given by eq 26. The generalized Darken relation (eq 26) has been verified by the MD simulations of ternary and quaternary mixtures of linear alkanes.

Further work is required to ascertain the validity of the Darken relation for liquid mixtures that contain polar molecules.

Acknowledgment

R.K. acknowledges two grants: *Programmasubsidie* and TOP subsidy from The Netherlands Foundation for Fundamental Research (NWO-CW) for the development of novel concepts in reactive separations technology and for intensification of reactors. We gratefully acknowledge D. Dubbeldam, S. Calero, T. J. H. Vlugt, E. Beerdsen, and B. Smit for providing the CBMC and MD simulation codes. We acknowledge NWO/NCF for the provision of high-performance computing resources in terms of PC clusters.

Supporting Information Available: The Darken relation for multicomponent diffusion in liquid mixtures. An investigation using MD simulations. Appendix A contains the complete set of data on $D_{i,\mathrm{self}}$ and $Đ_{ij}$ for each campaign listed in Table 1; Appendix B contains the detailed procedure for calculation of the M−S diffusivities $Đ_{ij}$ from the Onsager coefficients Λ_{ij} determined from MD simulations. (PDF.) This material is available free of charge via the Internet at http://pubs.acs.org.

Notation

a_i = activitity of species i (dimensionless)
$[B]$ = matrix of inverse Maxwell−Stefan coefficients (m^{-2} s)
$D_{i,\mathrm{self}}$ = self-diffusivity (m^2/s)
D_{12} = Fick diffusivity in binary mixture (m^2/s)
$Đ_{ij}$ = Maxwell-Stefan diffusivity of binary i−j pair (m^2/s)
M_i = molar mass of species i (kg/mol)
N_i = number of molecules of species i in the simulation box (dimensionless)
N = total number of molecules in the simulation box (dimensionless)
R = gas constant; R = 8.314 J mol^{-1} K^{-1}
t = time (s)
$\mathbf{u}$ = molar average mixture velocity (m/s)
$\mathbf{u}_i$ = ensemble-averaged velocity of species i (m/s)
$\mathbf{v}_i$ = velocity of species i (m/s)
x_i = mole fraction of species i (dimensionless)
T = absolute temperature (K)

Greek Letters

$[\Delta]$ = matrix of Maxwell-Stefan diffusivities (m^2/s)
γ_i = activity coefficient of species i (dimensionless)
ϕ_i = volume fraction of species i (dimensionless)
$[\Lambda]$ = matrix of Onsager coefficients (m^2/s)
μ_i = molar chemical potential of species i (J/mol)
ρ = density (kg/m^3)
ω_i = mass fraction of species i (dimensionless)

Subscripts

i, j = components in mixture

Superscripts

$x_i \to 1$ = parameter in mixture that contains species i predominantly

Vector and Matrix Notation

( ) = vector
[ ]= square matrix

Literature Cited

(1) Krishna, R.; Wesselingh, J. A. The Maxwell-Stefan approach to mass transfer. *Chem. Eng. Sci.* **1997**, *52*, 861−911.

(2) Taylor, R.; Krishna, R. *Multicomponent Mass Transfer*; Wiley: New York, New York, 1993.

(3) Wesselingh, J. A.; Krishna, R. *Mass Transfer in Multicomponent Mixtures*; Delft University Press: Delft, The Netherlands, 2000.

(4) Price, P. E.; Romdhane, I. H. Multicomponent diffusion theory and its applications to polymer−solvent systems. *AIChE J.* **2003**, *49*, 309−322.

(5) Wheeler, D. R.; Newman, J. Molecular dynamics simulations of multicomponent diffusion. 1. Equilibrium method. *J. Phys. Chem. B* **2004**, *108*, 18353−18361.

(6) Wheeler, D. R.; Newman, J. Molecular dynamics simulations of multicomponent diffusion. 2. Nonequilibrium method. *J. Phys. Chem. B* **2004**, *108*, 18362−18367.

(7) Mauviel, G.; Favre, E. Free-volume theory applied to diffusion in liquids: A critical analysis. *Ind. Eng. Chem. Res.* **2004**, *43*, 6847−6854.

(8) Darken, L. S. Diffusion, Mobility and Their Interrelation through Free Energy in Binary Metallic Systems. *Trans. Inst. Min. Metall. Eng.* **1948**, *175*, 184−201.

(9) Shieh, J. C.; Lyons, P. A. Transport Properties of Liquid *n*-Alkanes. *J. Phys. Chem.* **1969**, *73*, 3258−3264.

(10) Bidlack, D. L.; Anderson, D. K. Mutual diffusion in the system hexane−hexadecane. *J. Phys. Chem.* **1964**, *68*, 206−208.

(11) Helbaek, M.; Hafskjold, B.; Dysthe, D. K.; Sorland, G. H. Self-diffusion coefficients of methane or ethane mixtures with hydrocarbons at high pressure by NMR. *J. Chem. Eng. Data* **1996**, *41*, 598−603.

(12) Keffer, D. J.; Adhangale, P. The composition dependence of self-and transport diffusivities from molecular dynamics simulations. *Chem. Eng. J.* **2004**, *100*, 51−69.

(13) Keffer, D. J.; Edwards, B. J.; Adhangale, P. Determination of statistically reliable transport diffusivities from molecular dynamics simulation. *J. Non-Newtonian Fluid Mech.* **2004**, *120*, 41−53.

(14) Fernandez, G. A.; Vrabec, J.; Hasse, H. Self-diffusion and binary Maxwell-Stefan diffusion in simple fluids with the Green-Kubo method. *Int. J. Thermophys.* **2004**, *25*, 175−186.

(15) Merzliak, T.; Pfennig, A. Development of a model for the description of intra-diffusion in homogeneous liquid Lennard-Jones mixtures. *Mol. Simul.* **2004**, *30*, 459−468.

(16) Goo, G. H.; Sung, G. H.; Lee, S. H.; Chang, T. Y. Diffusion behavior of *n*-alkanes by molecular dynamics simulations. *Bull. Korean Chem. Soc.* **2002**, *23*, 1595−1603.

(17) Sharma, R.; Tankeshwar, K. Mutual diffusion in binary systems. *J. Chem. Phys.* **1998**, *108*, 2601−2607.

(18) Travis, K. P.; Brown, D.; Clarke, J. H. R. A Molecular-Dynamics Study of the Coupling of Torsional Motions to Self-Diffusion in Liquid N−Hexane. *J. Chem. Phys.* **1995**, *102*, 2174−2180.

(19) Harmandaris, V. A.; Angelopoulou, D.; Mavrantzas, V. G.; Theodorou, D. N. Atomistic molecular dynamics simulation of diffusion in binary liquid *n*-alkane mixtures. *J. Chem. Phys.* **2002**, *116*, 7656−7665.

(20) Dysthe, D. K.; Fuchs, A. H.; Rousseau, B. Fluid transport properties by equilibrium molecular dynamics. III. Evaluation of united atom interaction potential models for pure alkanes. *J. Chem. Phys.* **2000**, *112*, 7581−7590.

(21) Dysthe, D. K.; Fuchs, A. H.; Rousseau, B.; Durandeau, M. Fluid transport properties by equilibrium molecular dynamics. II. Multicomponent systems. *J. Chem. Phys.* **1999**, *110*, 4060−4067.

(22) Van de Ven-Lucassen, I. M. J. J.; Vlugt, T. J. H.; Van der Zanden, A. J. J.; Kerkhof, P. J. A. M. Using molecular dynamics to obtain Maxwell-Stefan diffusion coefficients in liquid systems. *Mol. Phys.* **1998**, *94*, 495−503.

(23) Frenkel, D.; Smit, B. *Understanding Molecular Simulations: From Algorithms to Applications*; Academic Press: San Diego, CA, 2002.

(24) Poling, B. E.; Prausnitz, J. M.; O'Connell, J. P. *The Properties of Gases and Liquids*; McGraw-Hill: New York, 2001.

(25) Li, J.; Liu, H. L.; Hu, Y. A mutual-diffusion-coefficient model based on local composition. *Fluid Phase Equilib.* **2001**, *187*, 193−208.

(26) Hsu, Y. D.; Tang, M.; Chen, Y. P. A group contribution correlation of the mutual diffusion coefficients of binary liquid mixtures. *Fluid Phase Equilib.* **2000**, *173*, 1−21.

(27) Hsu, Y. D.; Chen, Y. P. Correlation of the mutual diffusion coefficients of binary liquid mixtures. *Fluid Phase Equilib.* **1998**, *152*, 149−168.

(28) Yang, X. N. Determination of diffusion coefficients for binary nonelectrolyte mixtures. A free-volume predictive approach. *J. Solution Chem.* **1998**, *27*, 261−272.

(29) Yu, Y. X.; Gao, G. H. Lennard-Jones chain model for self-diffusion of *n*-alkanes. *Int. J. Thermophys.* **2000**, *21*, 57−70.

(30) Vignes, A. Diffusion in binary solutions. *Ind. Eng. Chem. Fundam.* **1966**, *5*, 189−199.

(31) He, C. Prediction of the concentration dependence of mutual diffusion coefficients in binary liquid mixtures. *Ind. Eng. Chem. Res.* **1995**, *34*, 2148−2153.

(32) Wesselingh, J. A.; Bollen, A. M. Multicomponent diffusivities from the free volume theory. *Chem. Eng. Res. Des.* **1997**, *75*, 590−602.

(33) Kooijman, H. A.; Taylor, R. Estimation of Diffusion-Coefficients in Multicomponent Liquid-Systems. *Ind. Eng. Chem. Res.* **1991**, *30*, 1217−1222.

(34) Krishna, R.; van Baten, J. M. Diffusion of alkane mixtures in zeolites. Validating the Maxwell-Stefan formulation using MD simulations. *J. Phys. Chem. B* **2005**, *109*, 6386−6396.

(35) Krishna, R.; Van Baten, J. M. Influence of isotherm inflection on the diffusivities of C5−C8 linear alkanes in MFI zeolite. *Chem. Phys. Lett.* **2005**, *407*, 159−165.

(36) Dubbeldam, D.; Calero, S.; Vlugt, T. J. H.; Krishna, R.; Maesen, T. L. M.; Beerdsen, E.; Smit, B. Force Field Parametrization through Fitting on Inflection Points in Isotherms. *Phys. Rev. Lett.* **2004**, *93* (8), Article No. 088302.

(37) Dubbeldam, D.; Calero, S.; Vlugt, T. J. H.; Krishna, R.; Maesen, T. L. M.; Smit, B. United Atom Force Field for Alkanes in Nanoporous Materials. *J. Phys. Chem. B* **2004**, *108*, 12301−12313.

(38) Buesche, F. *Physical Properties of Polymers*; Interscience: New York, 1962.

(39) von Meerwall, E.; Beckman, S.; Jang, J.; Mattice, W. L. Diffusion of liquid *n*-alkanes: Free-volume and density effects. *J. Chem. Phys.* **1998**, *108*, 4299−4304.

(40) von Meerwall, E.; Feick, E. J.; Ozisik, R.; Mattice, W. L. Diffusion in binary liquid *n*-alkane and alkane-polyethylene blends. *J. Chem. Phys.* **1999**, *111*, 750−757.

Received for review February 5, 2005
Revised manuscript received May 14, 2005
Accepted June 7, 2005

IE050146C

The Darken relation for multicomponent diffusion in liquid mixtures of linear alkanes. An investigation using MD simulations.

Supporting Information

R. Krishna and J.M. van Baten*

Van 't Hoff Institute for Molecular Sciences, University of Amsterdam, Nieuwe Achtergracht 166,

1018 WV Amsterdam, The Netherlands.

AUTHOR EMAIL ADDRESS. r.krishna@uva.nl

Contents:

Appendix A

- Contains data on $D_{i,self}$ and $Đ_{ij}$ for all the campaigns listed in Table 1 of the manuscript. The molecular loadings in the simulation box are also detailed here.
- The symbols represent the MD simulated data on $D_{i,self}$ and $Đ_{ij}$.
- The continuous solid lines represent calculations using the infinite dilution self diffusivities listed in Tables 3 and 4. The self-diffusivities in the various mixtures are calculated using Eq. (25) of the manuscript. The M-S diffusivities are calculated using the generalized Darken relation (26).

333 K; 30 MPa; linear alkanes, pure components

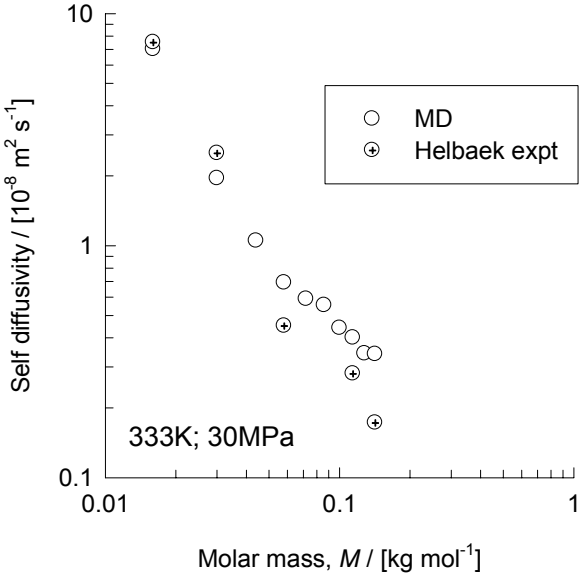

	Molar mass	Molecules in 25 Å box
C1	0.0160	110
C2	0.0301	134
C3	0.0441	117
nC4	0.0581	100
nC5	0.0722	84
nC6	0.0862	71
nC7	0.1002	63
nC8	0.1142	55
nC9	0.1283	50
nC10	0.1423	44

333 K; 30 MPa; C1-C2, C1-C3, and C2-C3 binary mixtures

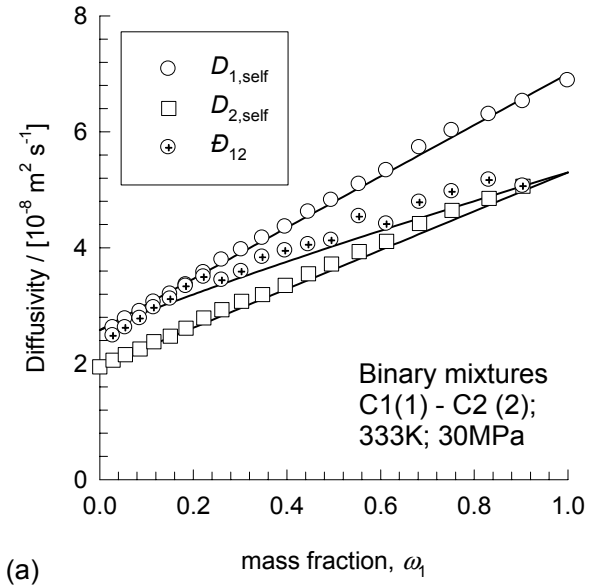

(a)

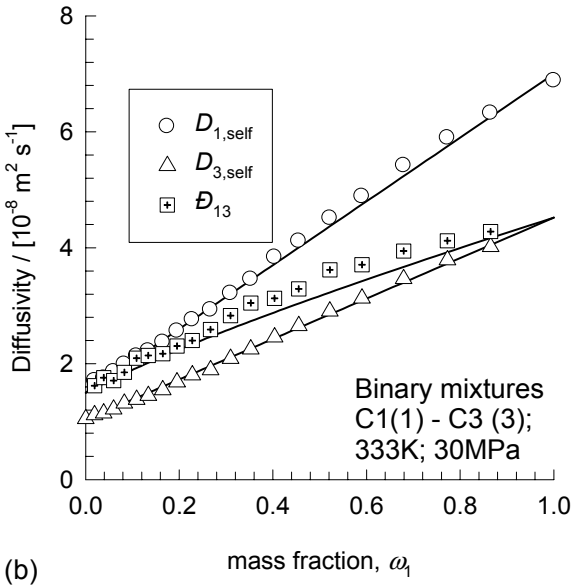

(b)

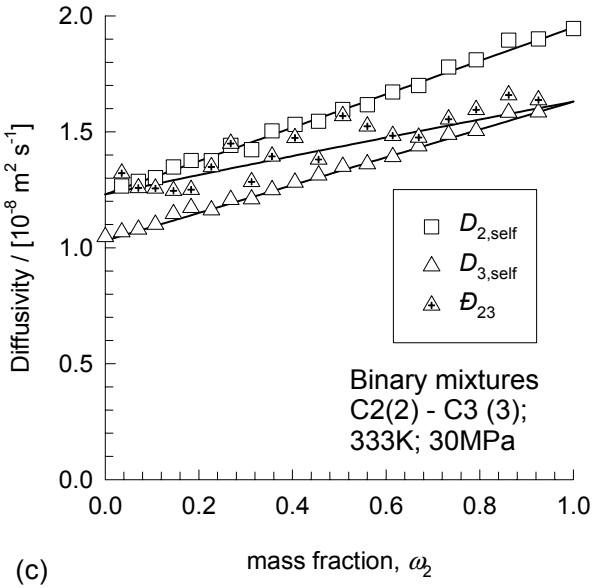

(c)

Molecules in 25 Å box	
C1	C2
0	134
7	127
13	120
20	113
26	106
33	99
39	92
45	84
51	77
57	70
63	63
69	56
74	49
79	43
84	36
89	30
93	23
97	17
102	11
106	6
110	0

Molecules in 25 Å box	
C1	C3
0	117
6	112
12	108
18	103
24	97
31	92
37	87
44	81
50	75
56	69
63	63
69	56
75	50
80	43
85	37
90	30
95	24
99	17
103	11
106	6
110	0

Molecules in 25 Å box	
C2	C3
0	117
6	112
12	107
18	102
24	96
30	91
37	86
43	80
50	75
56	69
63	63
70	57
77	51
84	45
91	39
98	33
105	26
112	20
119	13
127	7
134	0

333 K; 30 MPa; C1-C2-C3 ternary mixtures

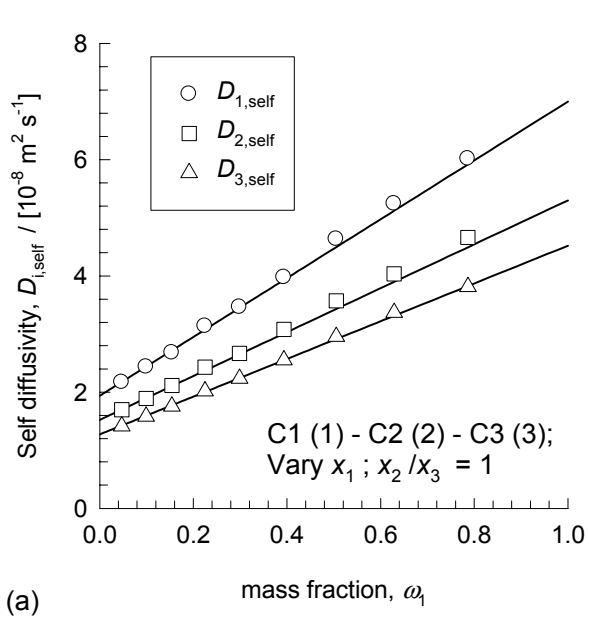

(a)

Molecules in 25 Å box		
C1	C2	C3
13	57	57
26	51	51
38	45	45
51	38	38
63	32	32
75	25	25
85	18	18
94	12	12
102	6	6

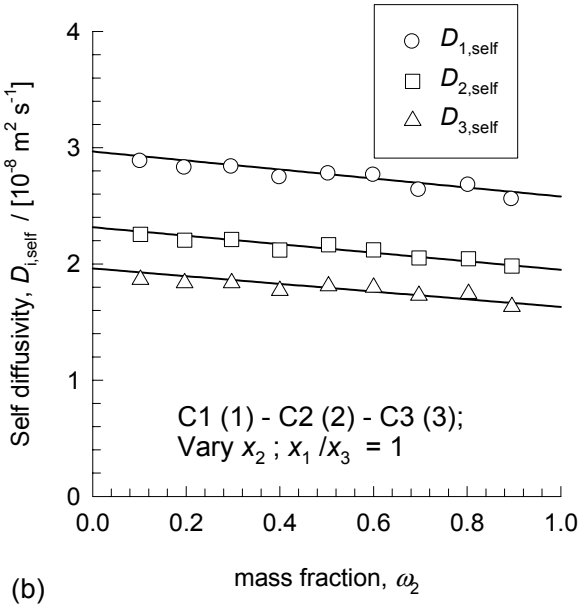

(b)

Molecules in 25 Å box		
C1	C2	C3
57	13	57
51	25	51
45	38	45
39	52	39
32	65	32
26	78	26
20	92	20
13	106	13
7	120	7

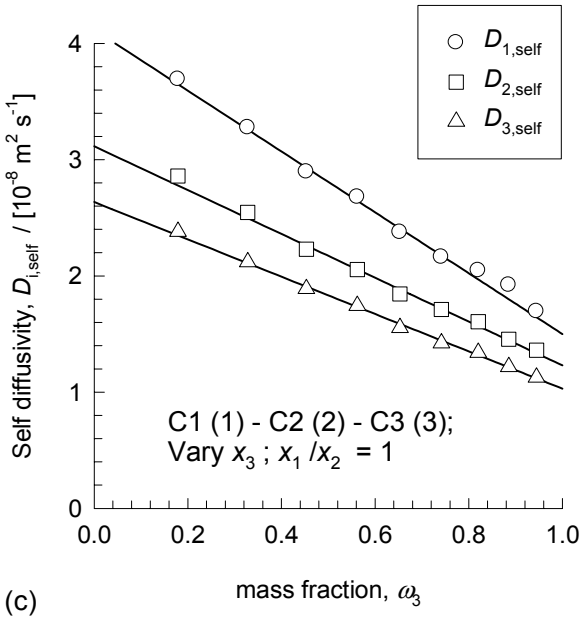

(c)

Molecules in 25 Å box		
C1	C2	C3
57	57	13
51	51	26
45	45	39
38	38	51
32	32	63
25	25	75
18	18	86
12	12	97
6	6	107

333 K; 30 MPa; C1-C2-C3 ternary mixtures

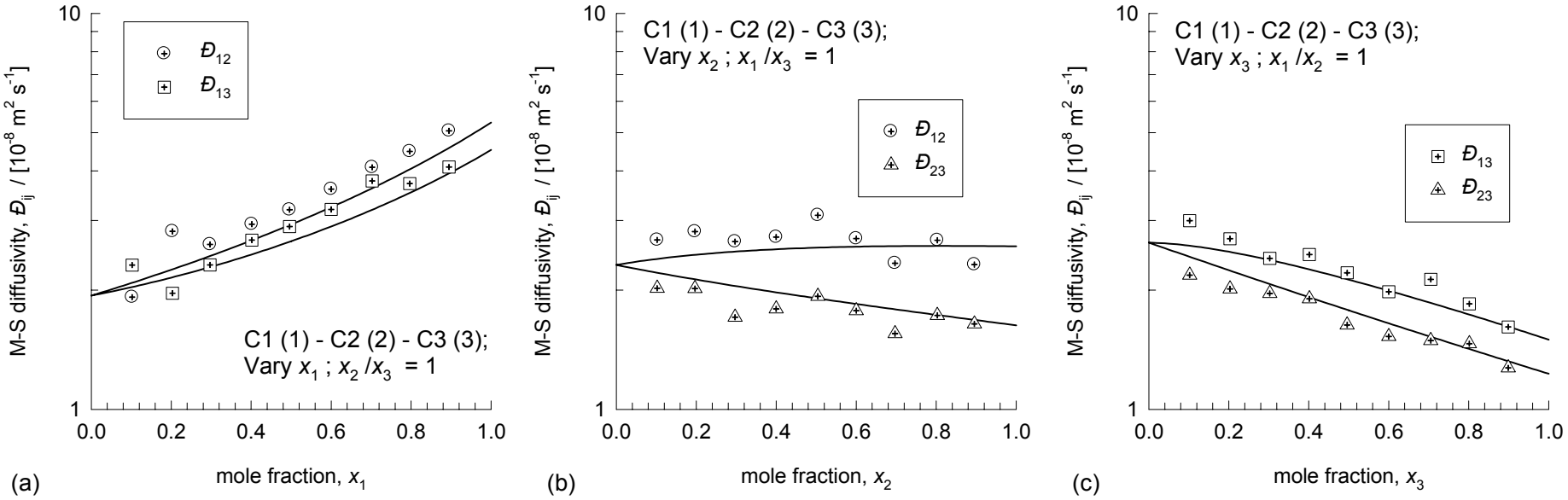

333 K; 30 MPa; C1-nC6: influence of simulation box size

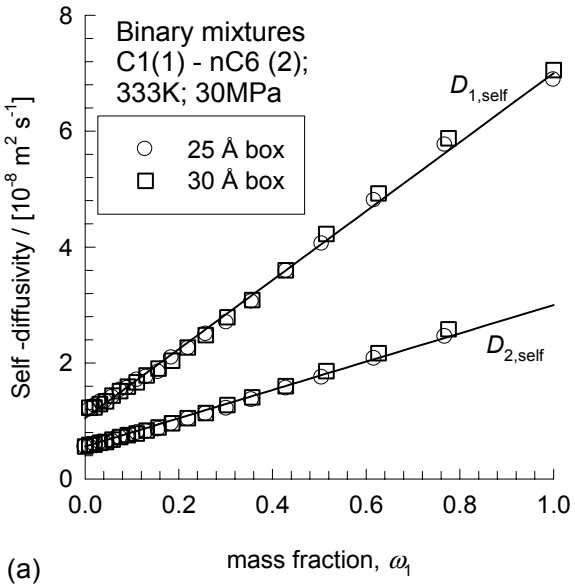

(a)

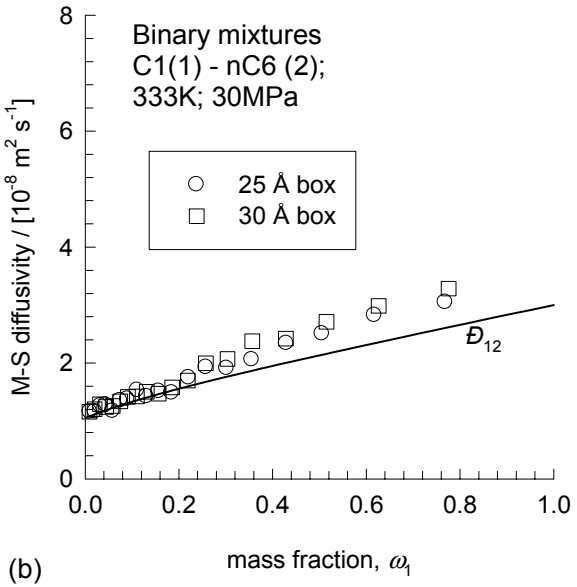

(b)

Molecules in 25 Å box	
C1	nC6
0	71
4	70
8	68
12	66
16	65
21	63
26	60
31	58
37	55
43	53
50	50
56	46
64	42
71	38
79	34
86	29
93	23
99	18
104	12
107	6
110	0

Molecules in 30 Å box	
C1	nC6
0	123
6	120
13	118
20	115
28	112
36	108
45	104
54	100
64	96
74	91
86	86
98	80
110	73
123	66
136	58
149	50
161	40
171	30
180	20
186	10
189	0

333 K; 30 MPa; C1-C2, C1-nC6, and C2-nC6 binary mixtures

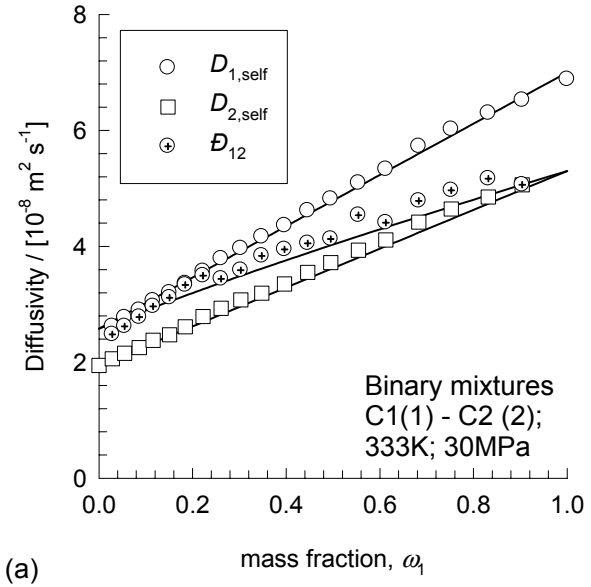

(a)

Molecules in 25 Å box	
C1	C2
0	134
7	127
13	120
20	113
26	106
33	99
39	92
45	84
51	77
57	70
63	63
69	56
74	49
79	43
84	36
89	30
93	23
97	17
102	11
106	6
110	0

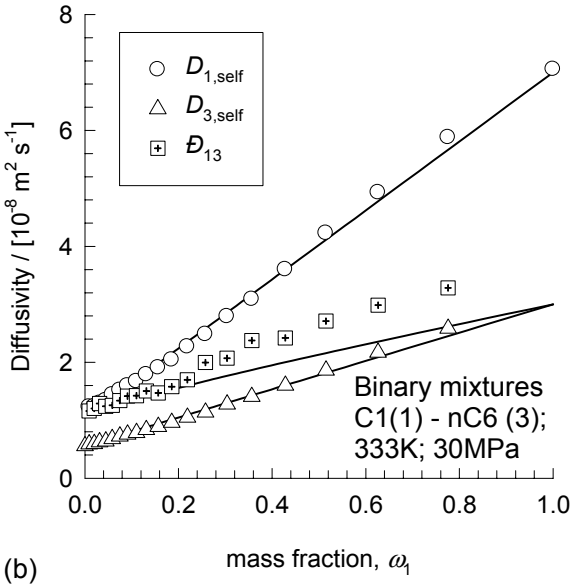

(b)

Molecules in 30 Å box	
C1	nC6
0	123
6	120
13	118
20	115
28	112
36	108
45	104
54	100
64	96
74	91
86	86
98	80
110	73
123	66
136	58
149	50
161	40
171	30
180	20
186	10
189	0

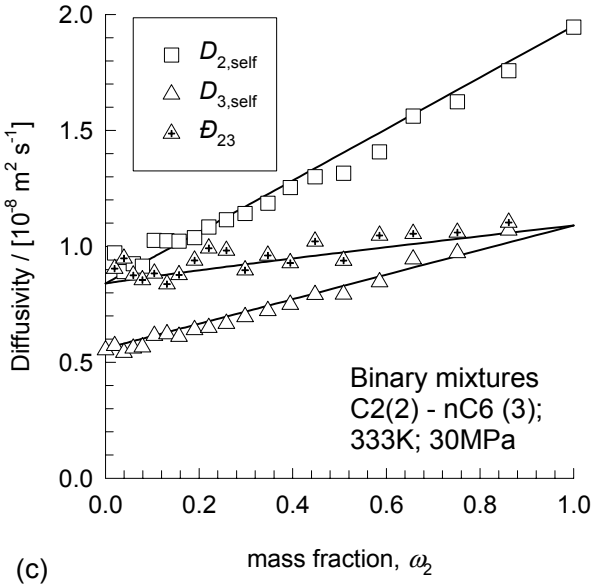

(c)

Molecules in 25 Å box	
C2	nC6
0	71
4	70
8	68
12	66
16	65
21	63
26	60
31	58
37	55
43	53
50	50
56	46
64	42
71	38
79	34
86	29
93	23
99	18
104	12
107	6
134	0

333 K; 30 MPa; C1-C2-nC6 ternary mixtures

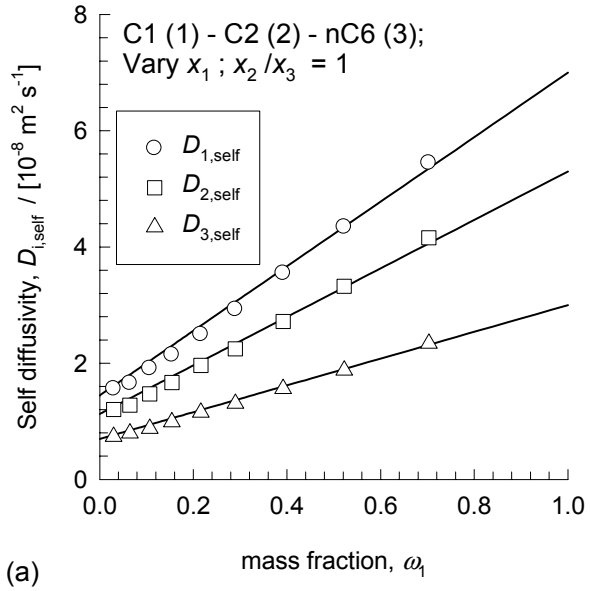

(a)

Molecules in 25 Å box		
C1	C2	nC6
10	45	45
21	42	42
33	38	38
45	34	34
58	29	29
71	24	24
84	18	18
95	12	12
103	6	6

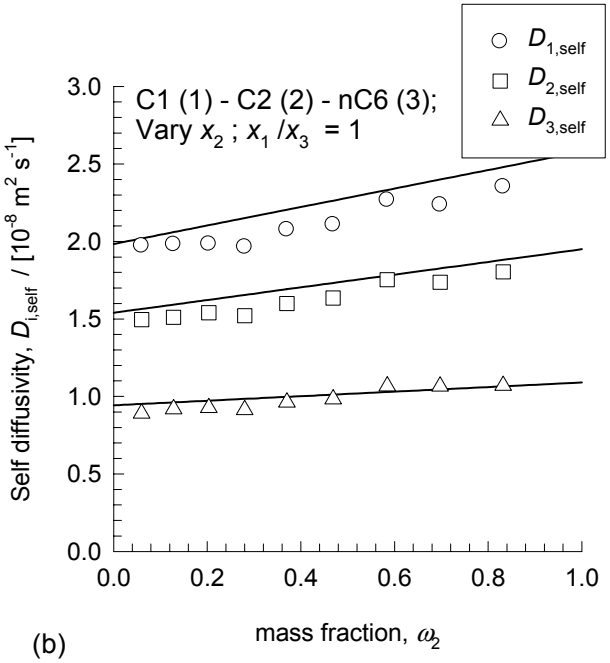

(b)

Molecules in 25 Å box		
C1	C2	nC6
46	10	46
42	21	42
38	33	38
34	45	34
29	58	29
24	72	24
18	86	18
13	102	13
7	118	7

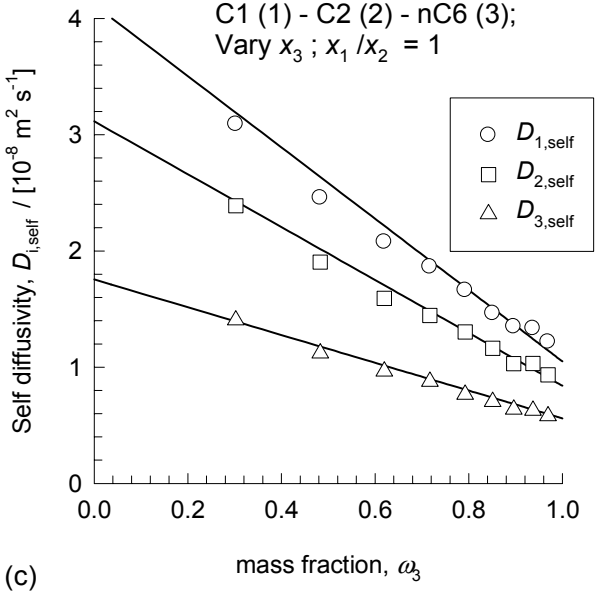

(c)

Molecules in 25 Å box		
C1	C2	nC6
56	56	13
48	48	24
39	39	34
31	31	42
24	24	49
18	18	55
13	13	60
8	8	64
4	4	68

333 K; 30 MPa; C1-C2-nC6 ternary mixtures

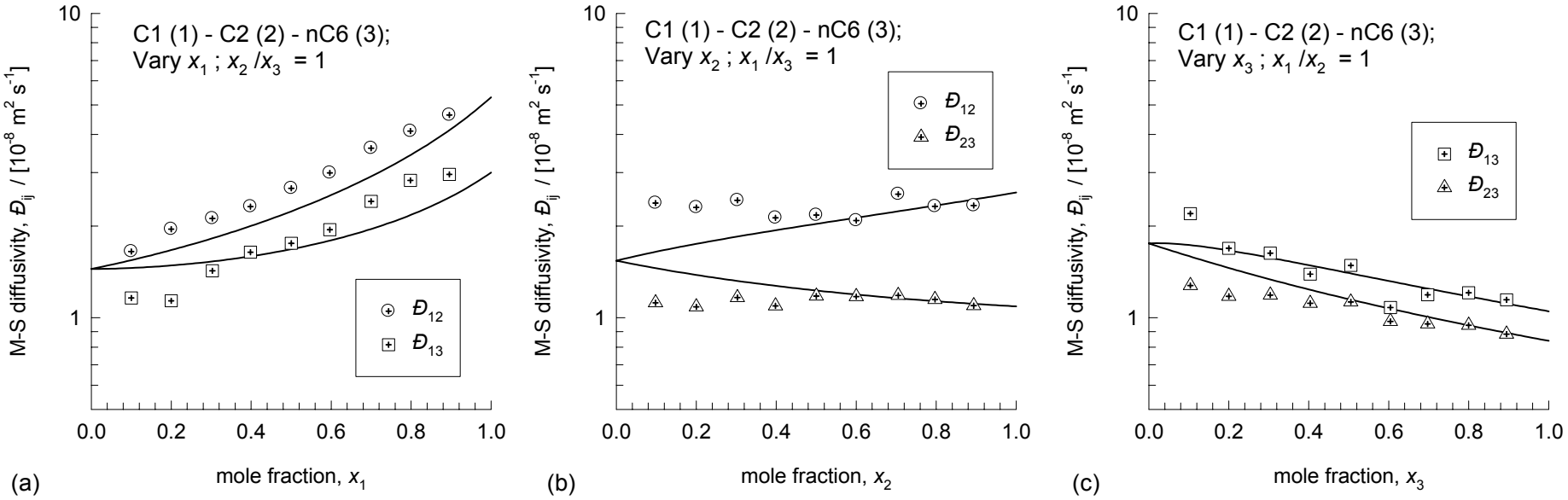

333 K; 50 MPa; C1-C2, C1-nC6, and C2-nC6 binary mixtures

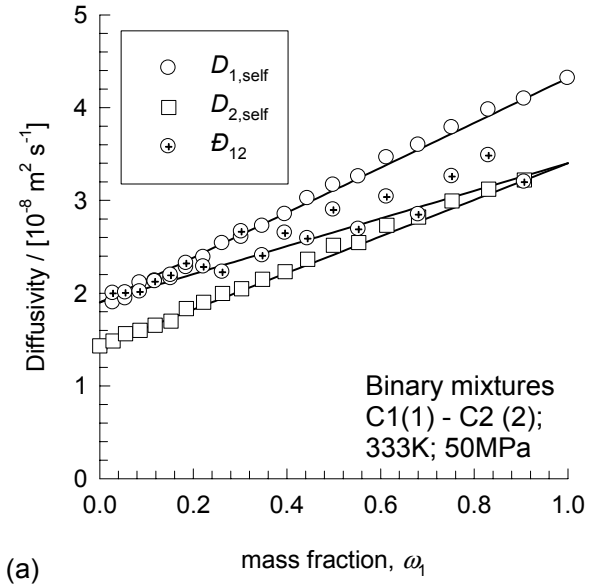

(a)

Molecules in 25 Å box	
C1	C2
	151
8	144
15	137
23	130
31	123
39	116
46	108
54	101
62	93
70	86
78	78
86	70
93	62
101	54
109	47
116	39
124	31
131	23
138	15
146	8
153	0

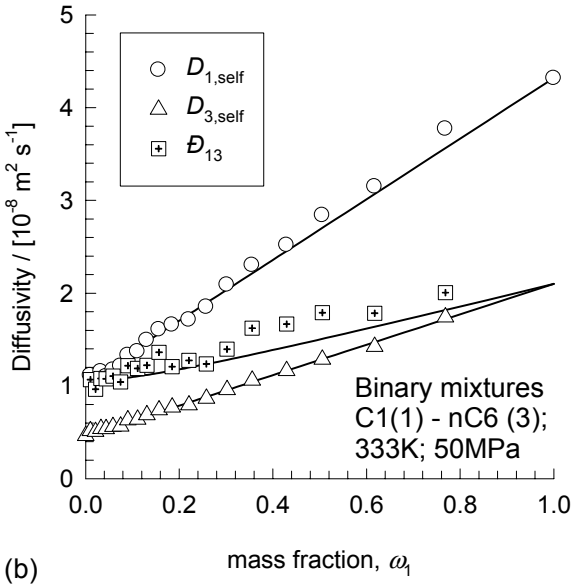

(b)

Molecules in 25 Å box	
C1	nC6
0	73
4	71
8	70
12	68
17	67
22	65
27	63
33	60
39	58
45	55
52	52
60	49
69	46
78	42
87	37
97	32
108	27
119	21
131	15
142	7
153	0

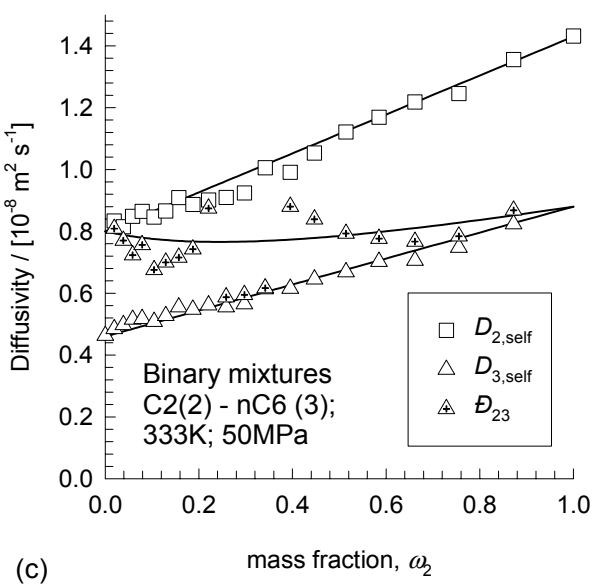

(c)

Molecules in 25 Å box	
C2	nC6
0	73
4	71
8	69
12	67
16	65
21	63
26	61
31	58
37	56
43	53
50	50
57	47
64	43
73	39
81	35
91	30
101	25
112	20
124	14
137	7
151	

333 K; 50 MPa; C1-C2-nC6 ternary mixtures

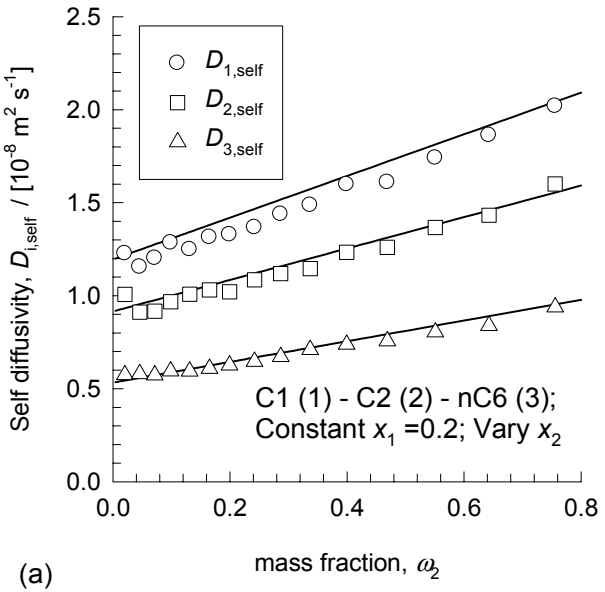

(a)

Molecules in 25 Å box		
C1	C2	C6
17	4	64
18	9	62
18	14	60
19	19	57
20	25	54
20	31	51
21	37	48
22	44	44
23	51	40
24	59	36
25	68	31
26	78	26
27	88	20
28	99	14
29	110	7

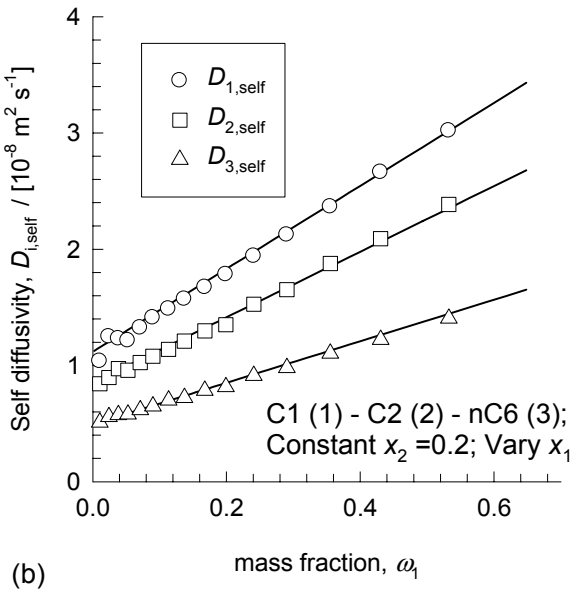

(b)

Molecules in 25 Å box		
C1	C2	C6
4	17	64
9	18	61
14	18	59
19	19	57
25	20	54
31	21	51
38	21	48
45	22	45
53	23	41
61	25	37
70	26	32
80	27	27
91	28	21
102	29	15
113	30	8

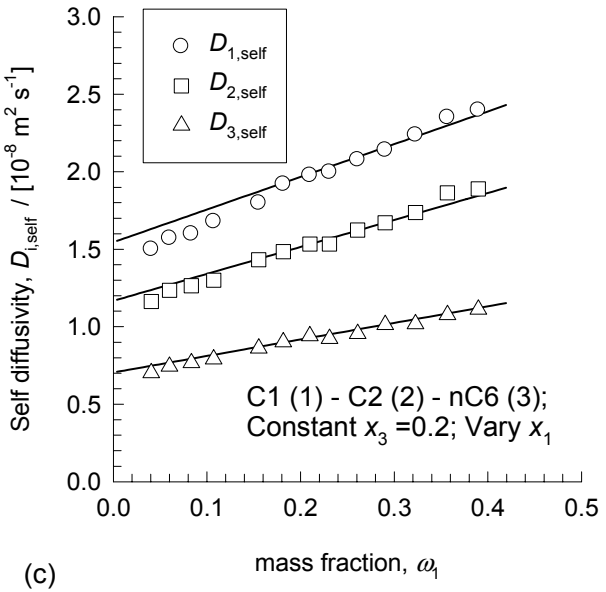

(c)

Molecules in 25 Å box		
C1	C2	C6
6	95	25
13	90	26
19	84	26
26	78	26
33	72	26
39	65	26
46	59	26
53	53	26
60	46	26
66	40	27
73	33	27
80	27	27
87	20	27
94	13	27
101	7	27

333 K; 30 MPa; C1-C3, C1-nC6, and C3-nC6 binary mixtures

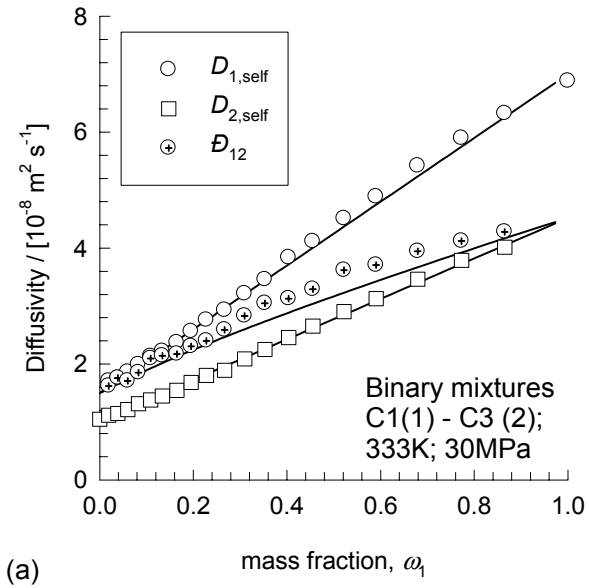

(a)

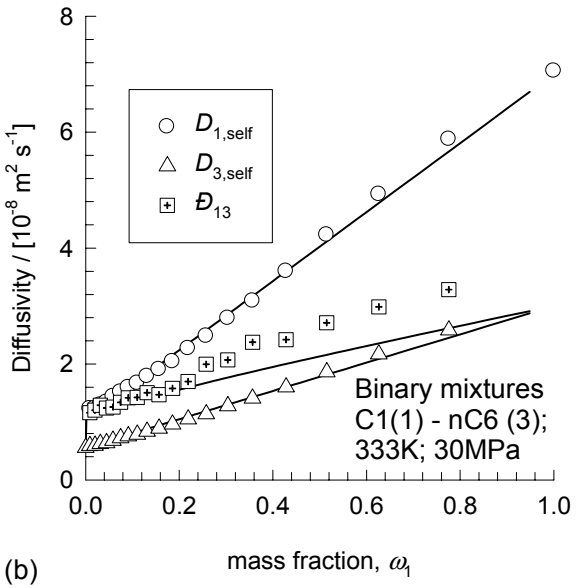

(b)

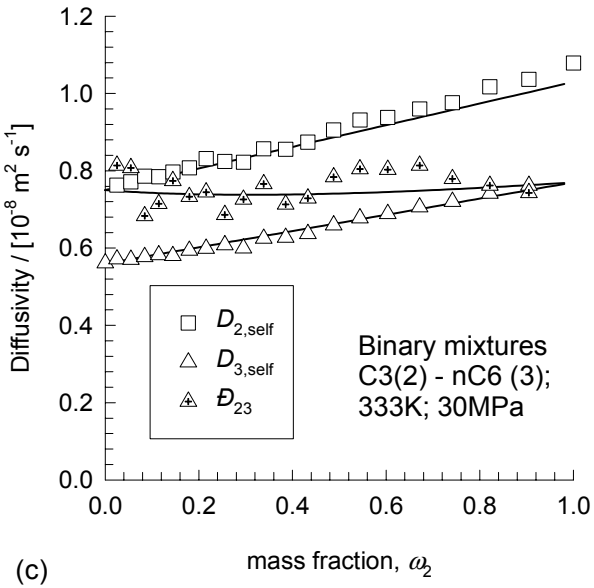

(c)

Molecules in 25 Å box	
C1	C3
0	117
6	112
12	108
18	103
24	97
31	92
37	87
44	81
50	75
56	69
63	63
69	56
75	50
80	43
85	37
90	30
95	24
99	17
103	11
106	6
110	0

Molecules in 30 Å box	
C1	nC6
0	123
6	120
13	118
20	115
28	112
36	108
45	104
54	100
64	96
74	91
86	86
98	80
110	73
123	66
136	58
149	50
161	40
171	30
180	20
186	10
189	0

Molecules in 30 Å box	
C3	nC6
0	123
6	119
13	115
20	111
27	107
34	103
42	98
50	93
59	88
68	83
77	77
87	71
97	65
108	58
119	51
131	44
144	36
157	28
171	19
186	10
202	0

333 K; 30 MPa; C1-C3-nC6 ternary mixtures

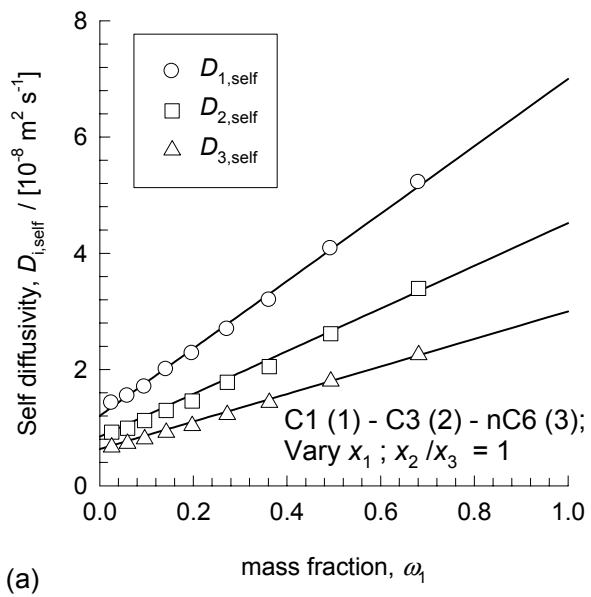

(a)

Molecules in 25 Å box		
C1	C3	nC6
9	42	42
20	39	39
31	36	36
43	32	32
56	28	28
70	23	23
83	18	18
95	12	12
104	6	6

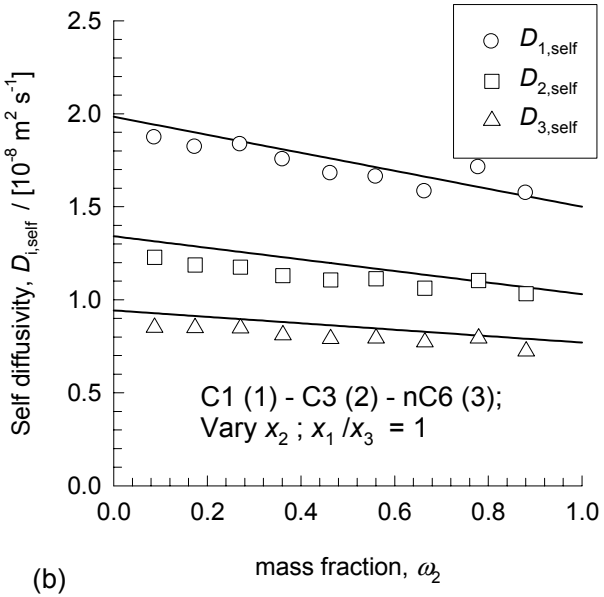

(b)

Molecules in 25 Å box		
C1	C3	nC6
45	10	45
41	20	41
36	31	36
32	42	32
27	54	27
22	65	22
17	78	17
11	90	11
6	103	6

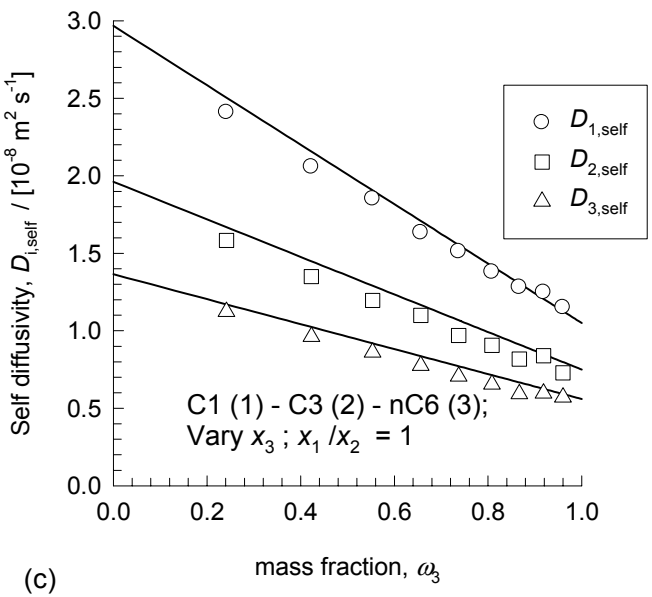

(c)

Molecules in 25 Å box		
C1	C3	nC6
54	54	12
45	45	23
37	37	32
30	30	40
24	24	47
18	18	53
13	13	59
8	8	63
4	4	67

333 K; 30 MPa; C1-C3-nC6 ternary mixtures

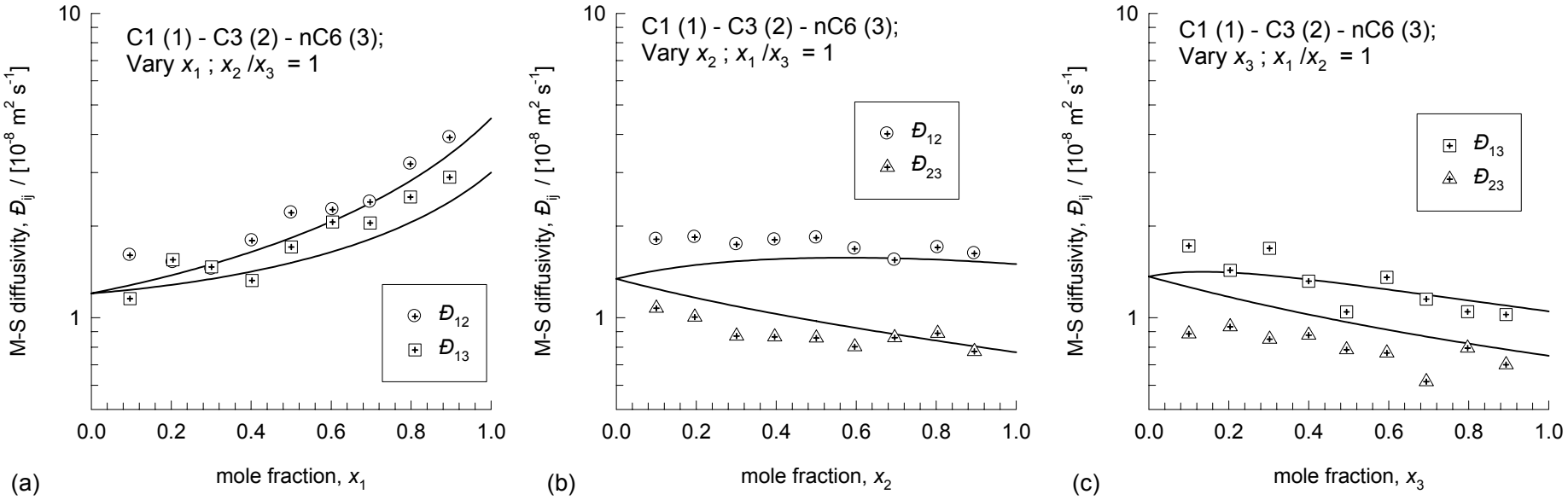

333 K; 30 MPa; C2-C3, C2-nC4, and C3-nC4 binary mixtures

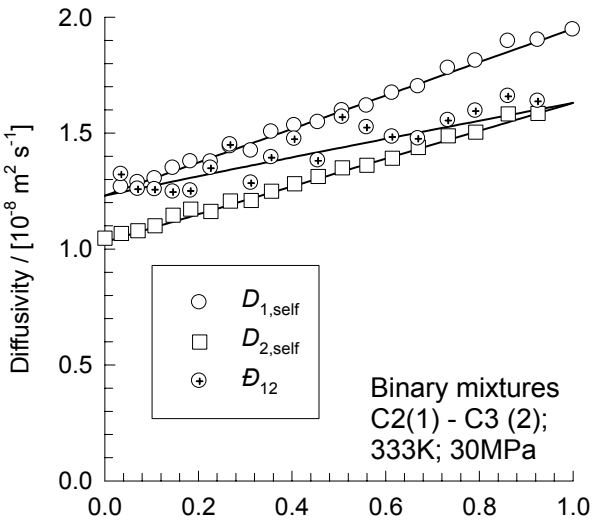

(a)

Molecules in 25 Å box	
C2	C3
0	117
6	112
12	107
18	102
24	96
30	91
37	86
43	80
50	75
56	69
63	63
70	57
77	51
84	45
91	39
98	33
105	26
112	20
119	13
127	7
134	0

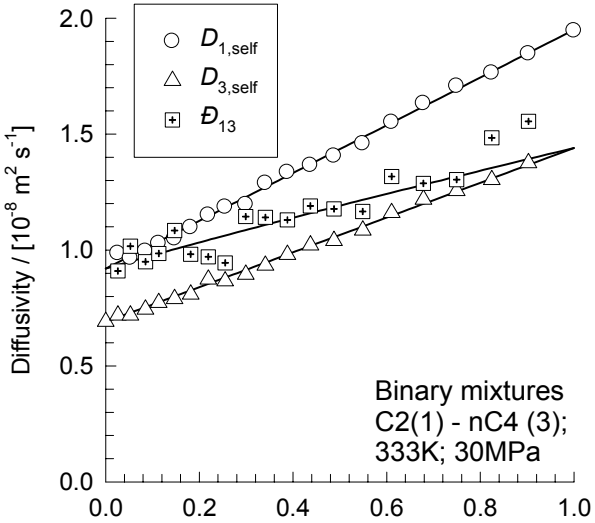

(b)

Molecules in 25 Å box	
C2	nC4
0	100
5	96
10	93
16	89
21	85
27	81
33	77
39	72
45	68
52	63
58	58
65	53
72	48
79	43
87	37
94	31
102	25
110	19
118	13
126	7
134	0

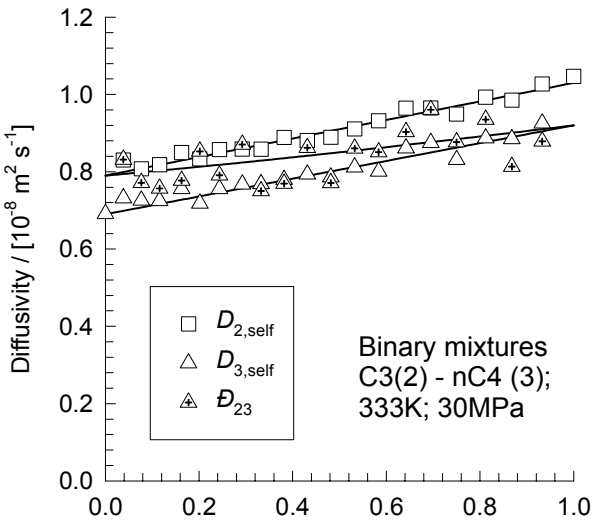

(c)

Molecules in 25 Å box	
C3	nC4
0	100
5	95
10	91
15	87
21	82
26	78
31	73
37	68
42	64
48	59
54	54
60	49
66	44
72	39
78	33
84	28
91	23
97	17
104	12
110	6
134	0

333 K; 30 MPa; C2-C3-nC4 ternary mixtures

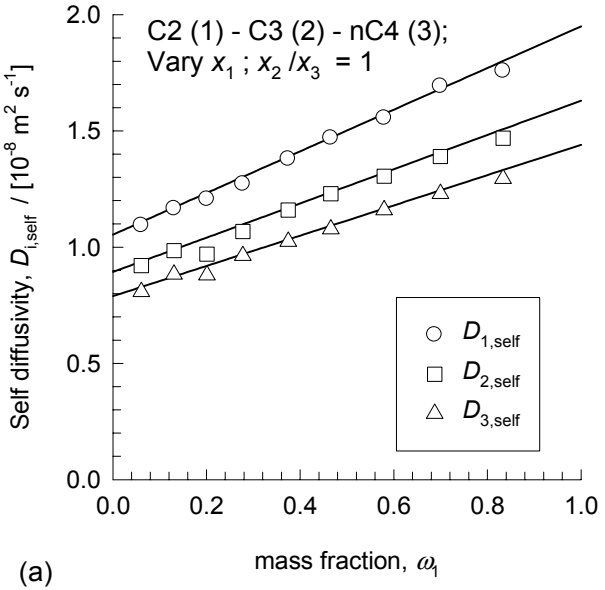

(a)

Molecules in 25 Å box		
C2	C3	nC4
11	50	50
23	45	45
35	41	41
47	36	36
61	30	30
74	25	25
89	19	19
103	13	13
119	7	7

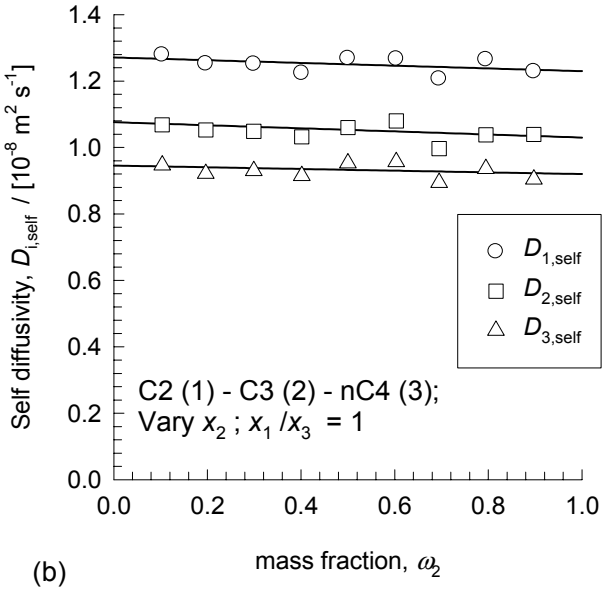

(b)

Molecules in 25 Å box		
C2	C3	nC4
52	12	52
47	23	47
41	35	41
35	47	35
29	58	29
23	70	23
18	82	18
12	93	12
6	105	6

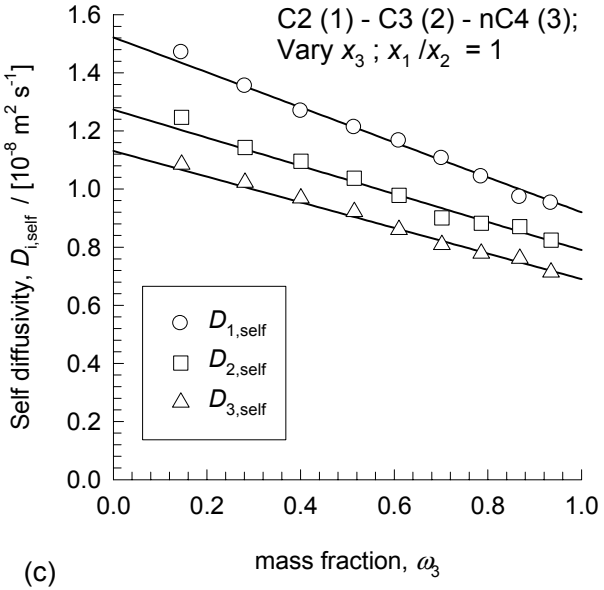

(c)

Molecules in 25 Å box		
C2	C3	nC4
55	55	12
48	48	24
41	41	35
34	34	46
28	28	56
22	22	66
16	16	75
10	10	84
5	5	92

333 K; 30 MPa; C2-C3-nC4 ternary mixtures

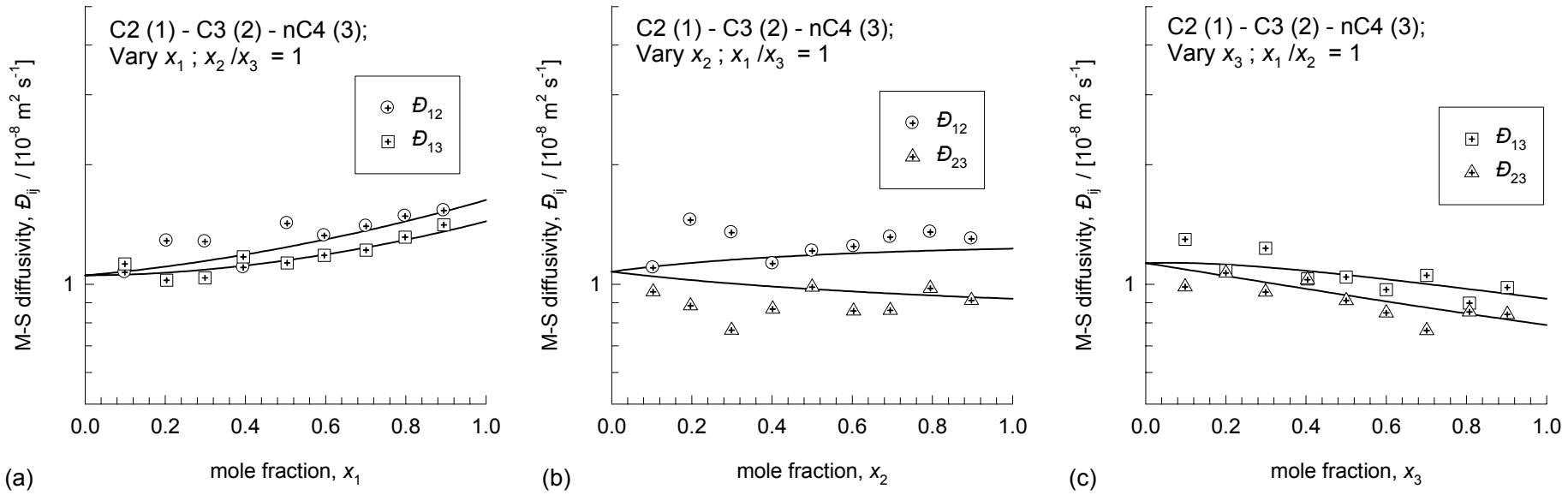

333 K; 30 MPa; C3-nC4, C3-nC5, and nC4-nC5 binary mixtures

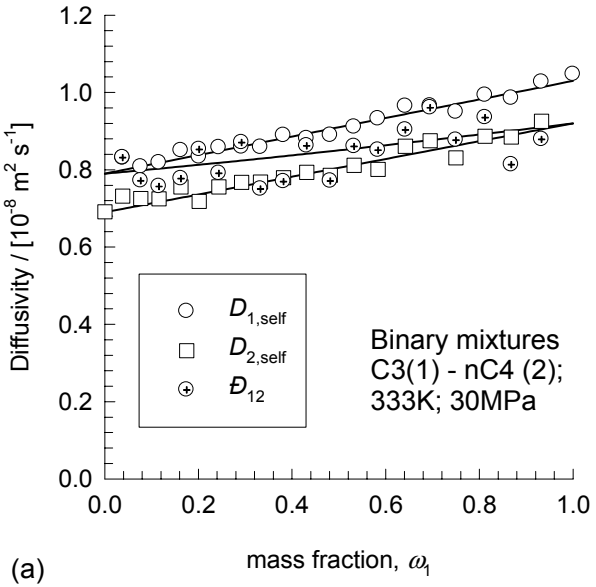

(a)

Molecules in 25 Å box	
C3	nC4
0	100
5	95
10	91
15	87
21	82
26	78
31	73
37	68
42	64
48	59
54	54
60	49
66	44
72	39
78	33
84	28
91	23
97	17
104	12
110	6
134	0

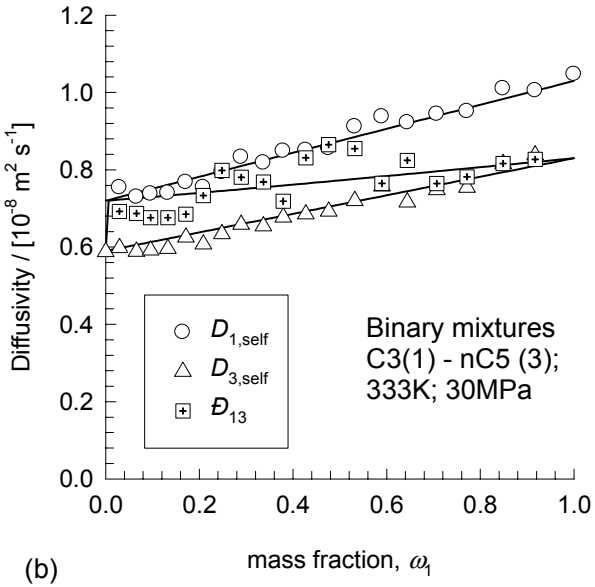

(b)

C3	nC5
0	84
4	81
9	78
13	75
18	72
23	68
28	65
33	61
38	57
44	53
49	49
55	45
61	41
67	36
73	31
80	27
87	22
94	17
101	11
109	6
134	0

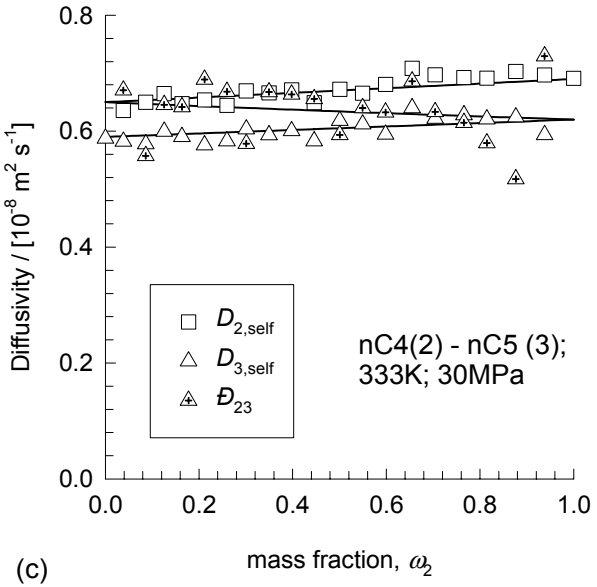

(c)

Molecules in 25 Å box	
nC4	nC5
0	84
4	81
9	77
13	73
17	70
22	66
27	62
31	58
36	54
41	50
46	46
51	41
56	37
61	33
66	28
71	24
77	19
82	15
88	10
94	5
100	0

333 K; 30 MPa; C3-nC4-nC5 ternary mixtures

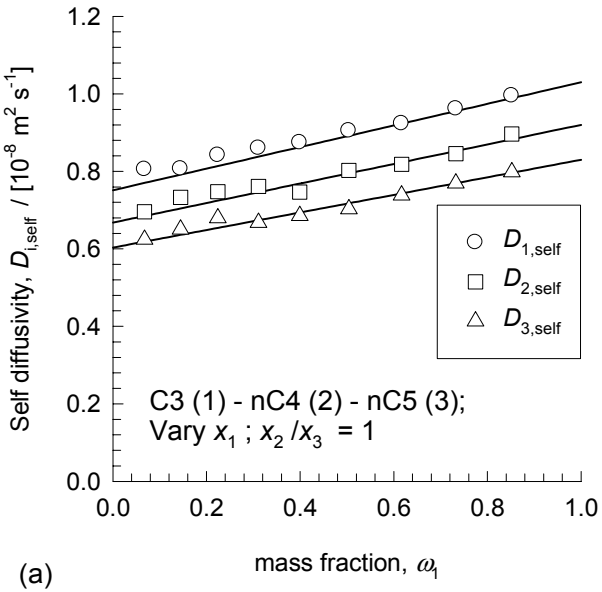

(a)

Molecules in 25 Å box		
C3	nC4	nC5
9	42	42
19	38	38
29	34	34
40	30	30
51	26	26
63	21	21
76	16	16
89	11	11
102	6	6

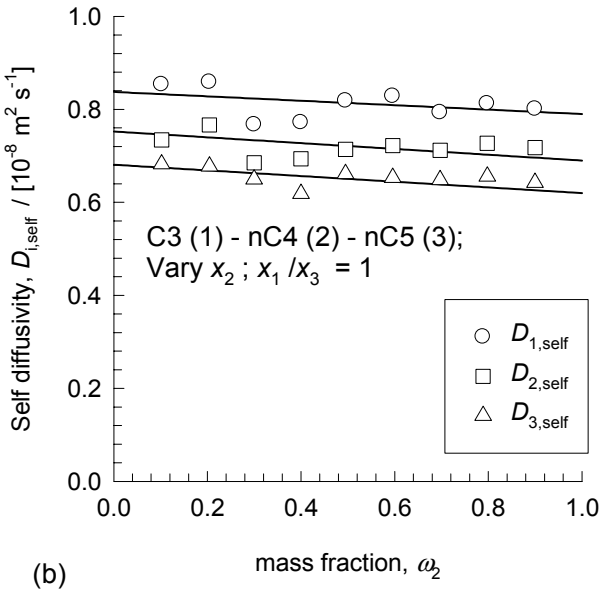

(b)

Molecules in 25 Å box		
C3	nC4	nC5
44	10	44
39	20	39
35	30	35
30	40	30
25	49	25
20	59	20
15	69	15
10	79	10
5	90	5

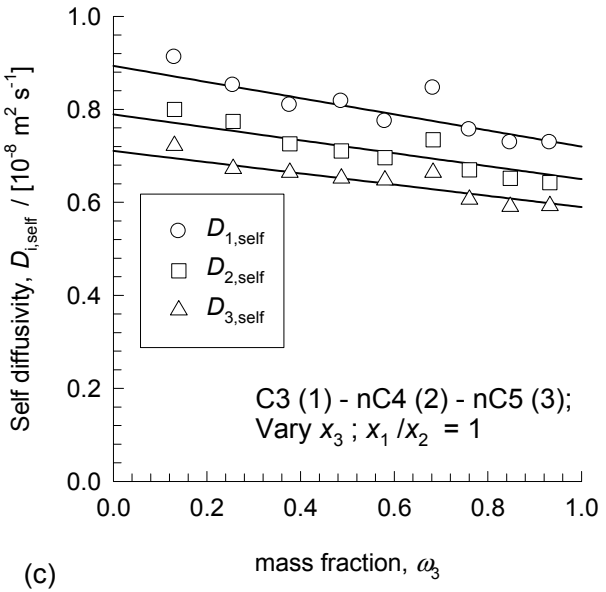

(c)

Molecules in 25 Å box		
C3	nC4	nC5
47	47	10
41	41	20
35	35	30
29	29	39
24	24	47
18	18	55
14	14	63
9	9	71
4	4	78

333 K; 30 MPa; C3-nC4-nC5 ternary mixtures

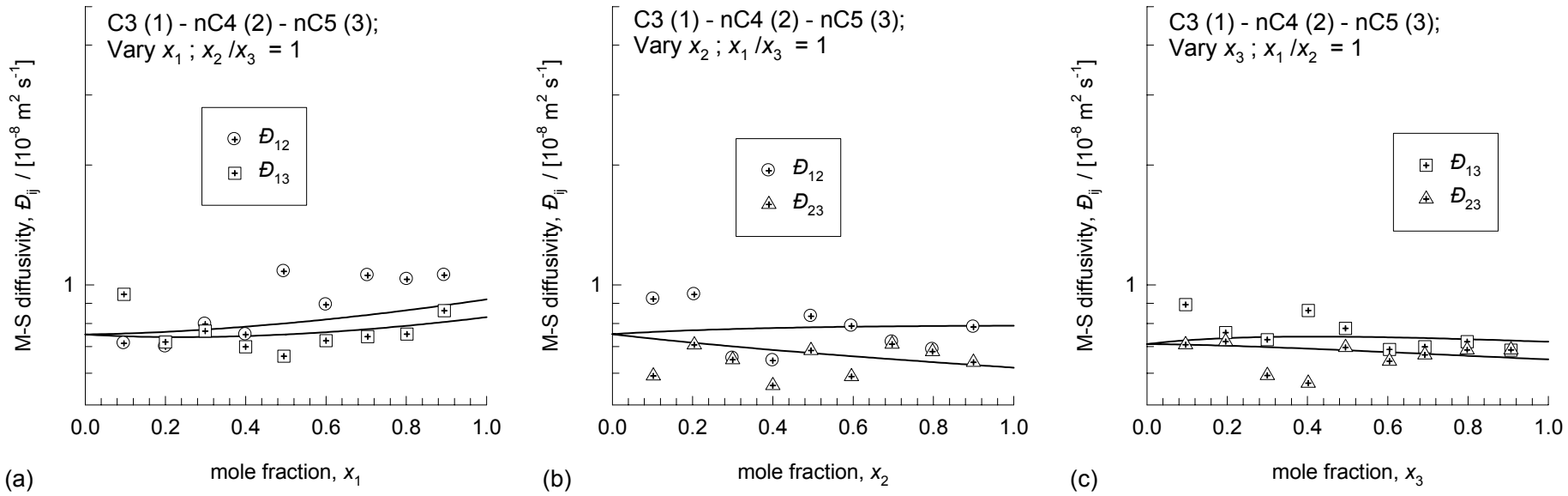

333 K; 30 MPa; C1-nC6, C1-nC8, and C1-nC10 binary mixtures

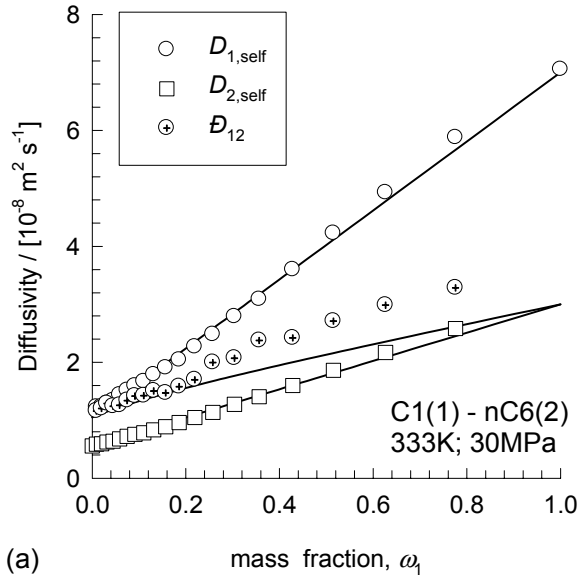

(a)

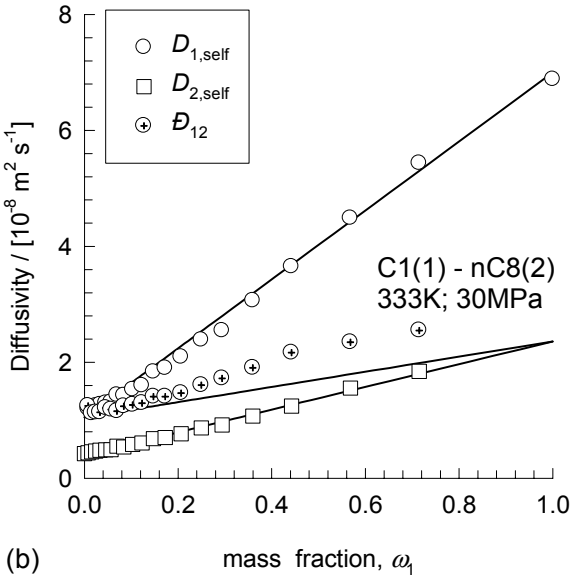

(b)

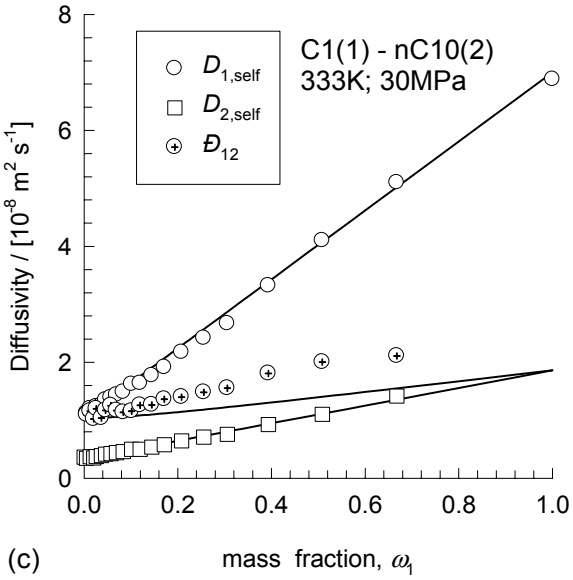

(c)

Molecules in 30 Å box

C1	nC6
0	123
6	120
13	118
20	115
28	112
36	108
45	104
54	100
64	96
74	91
86	86
98	80
110	73
123	66
136	58
149	50
161	40
171	30
180	20
186	10
189	0

Molecules in 25 Å box

C1	nC8
0	55
3	54
6	53
9	52
13	51
17	50
21	49
25	47
30	46
36	44
42	42
48	39
55	37
63	34
71	30
80	27
88	22
96	17
103	11
107	6
110	0

Molecules in 25 Å box

C1	nC10
0	44
2	44
5	43
8	43
10	42
14	41
17	40
21	39
25	38
30	37
35	35
41	34
48	32
55	30
63	27
73	24
82	21
92	16
101	11
107	6
110	0

333 K; 30 MPa; C2-nC6, C2-nC8, and C2-nC10 binary mixtures

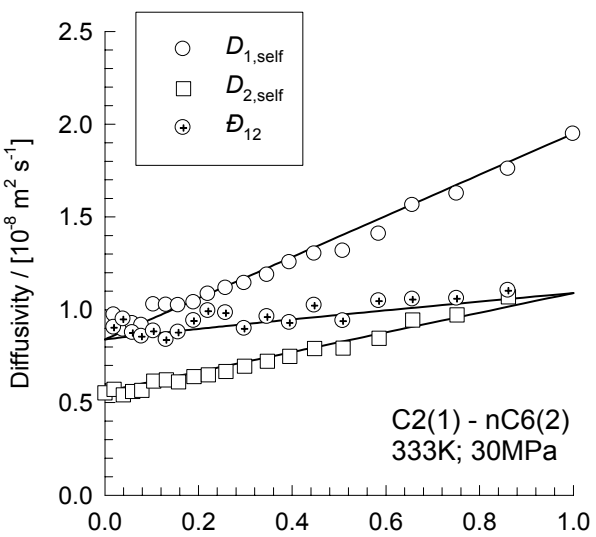

(a)

Molecules in 25 Å box	
C2	nC6
0	71
4	70
8	68
12	66
16	65
21	63
26	60
31	58
37	55
43	53
50	50
56	46
64	42
71	38
79	34
86	29
93	23
99	18
104	12
107	6
134	0

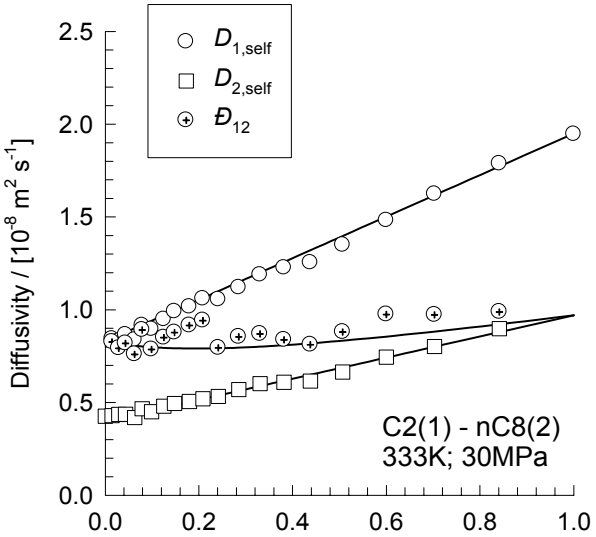

(b)

Molecules in 25 Å box	
C2	nC8
0	55
3	54
6	53
9	52
13	51
16	49
20	48
25	46
29	44
35	42
40	40
46	38
53	35
60	32
68	29
77	26
86	22
97	17
108	12
121	6
134	0

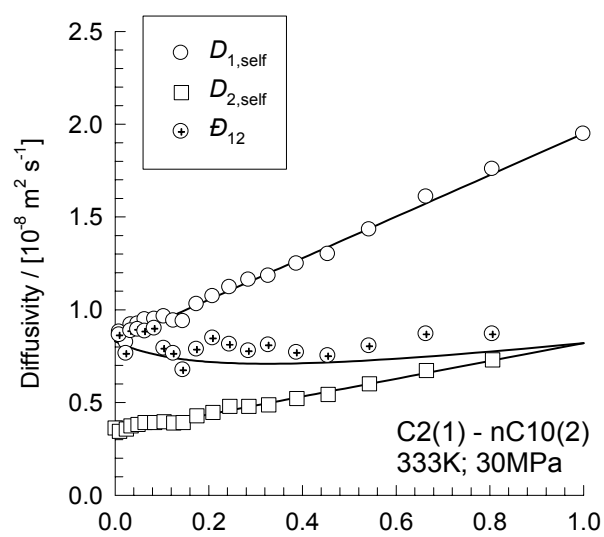

(c)

Molecules in 25 Å box	
C2	nC10
0	44
2	44
5	43
7	42
10	41
13	40
17	39
21	38
25	37
29	36
34	34
40	32
46	30
53	28
60	26
69	23
79	20
90	16
103	11
118	6
134	0

333 K; 30 MPa; C1-nC4 binary mixture

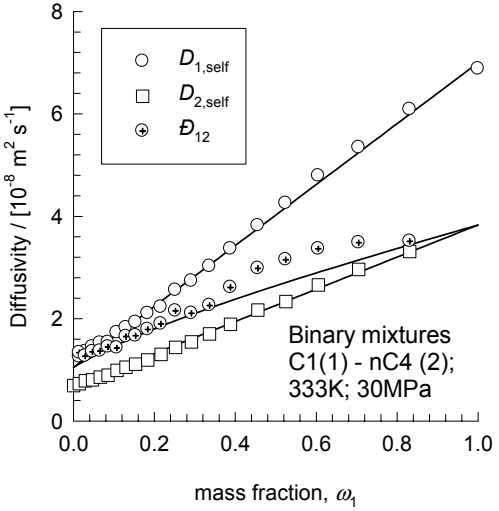

Molecules in 25 Å box	
C1	nC4
0	117
5	97
10	93
16	90
22	86
28	83
34	78
40	74
46	70
53	65
60	60
66	54
73	49
79	43
85	37
91	30
96	24
100	18
104	12
107	6
110	0

333 K; 30 MPa; C1-C2-C3-nC4 quaternary mixtures

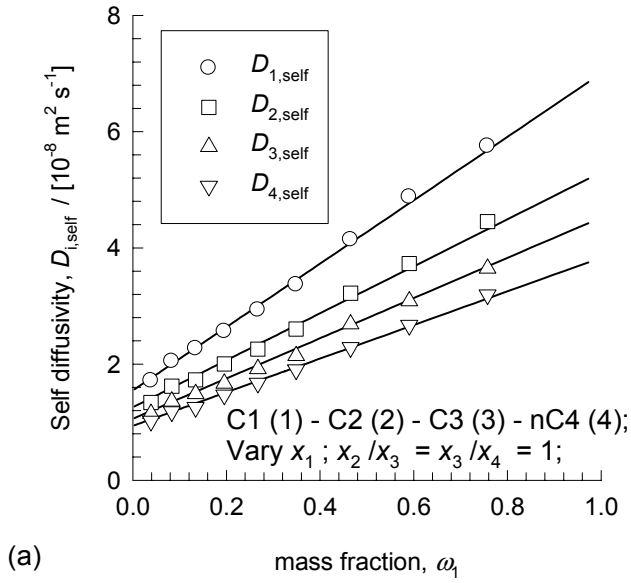

(a)

Molecules in 25 Å box			
C1	C2	C3	nC4
12	36	36	36
24	32	32	32
37	29	29	29
50	25	25	25
63	21	21	21
75	17	17	17
86	12	12	12
95	8	8	8
103	4	4	4

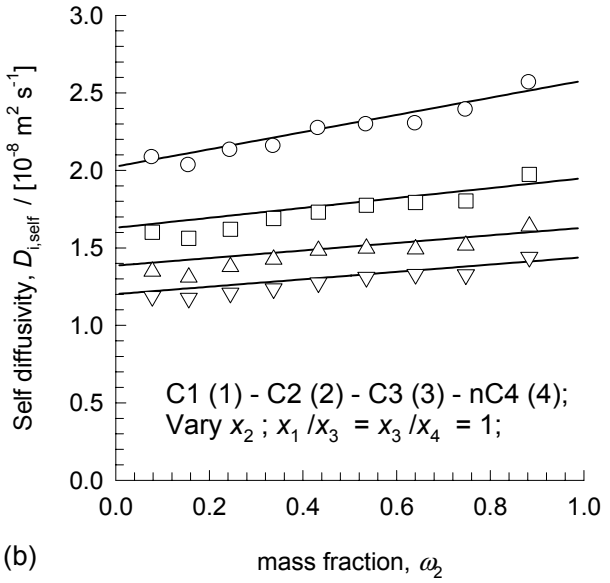

(b)

Molecules in 25 Å box			
C1	C2	C3	nC4
36	12	36	36
33	24	33	33
29	37	29	29
25	50	25	25
21	63	21	21
17	77	17	17
13	91	13	13
9	105	9	9
4	119	4	4

333 K; 30 MPa; C1-C2-C3-nC4 quaternary mixtures

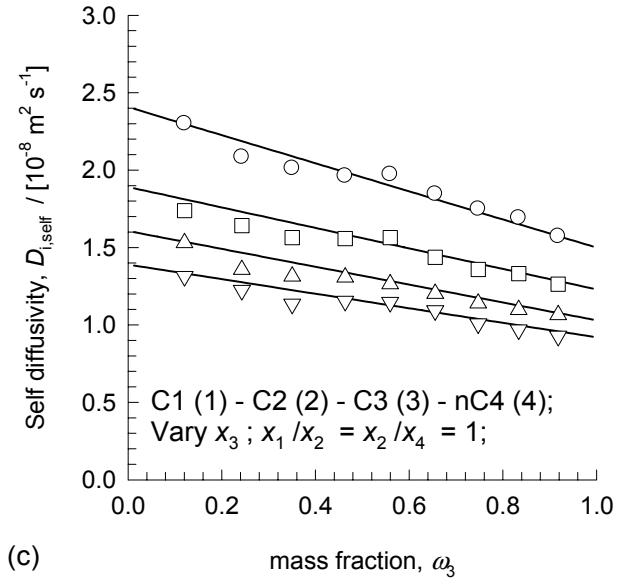

(c)

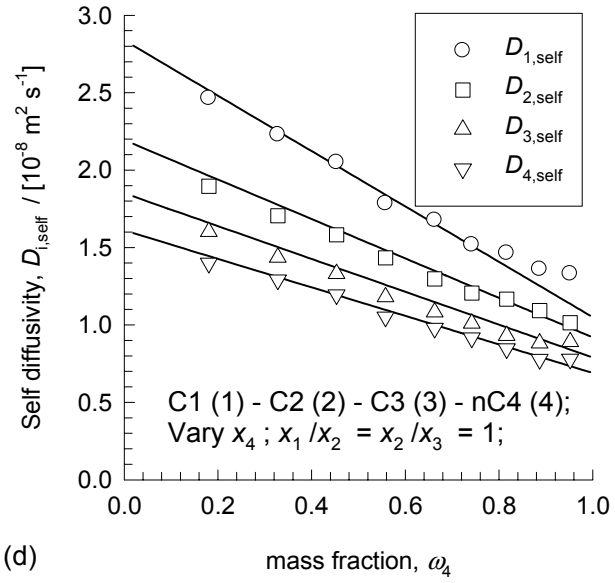

(d)

Molecules in 25 Å box			
C1	C2	C3	nC4
37	37	12	37
33	33	25	33
29	29	37	29
24	24	49	24
20	20	60	20
16	16	72	16
12	12	84	12
8	8	95	8
4	4	106	4

Molecules in 25 Å box			
C1	C2	C3	nC4
38	38	38	13
33	33	33	25
28	28	28	36
24	24	24	47
19	19	19	58
15	15	15	67
11	11	11	76
7	7	7	85
3	3	3	92

333 K; 30 MPa; C1-C2-C3-nC4 quaternary mixtures; M-S diffusivities

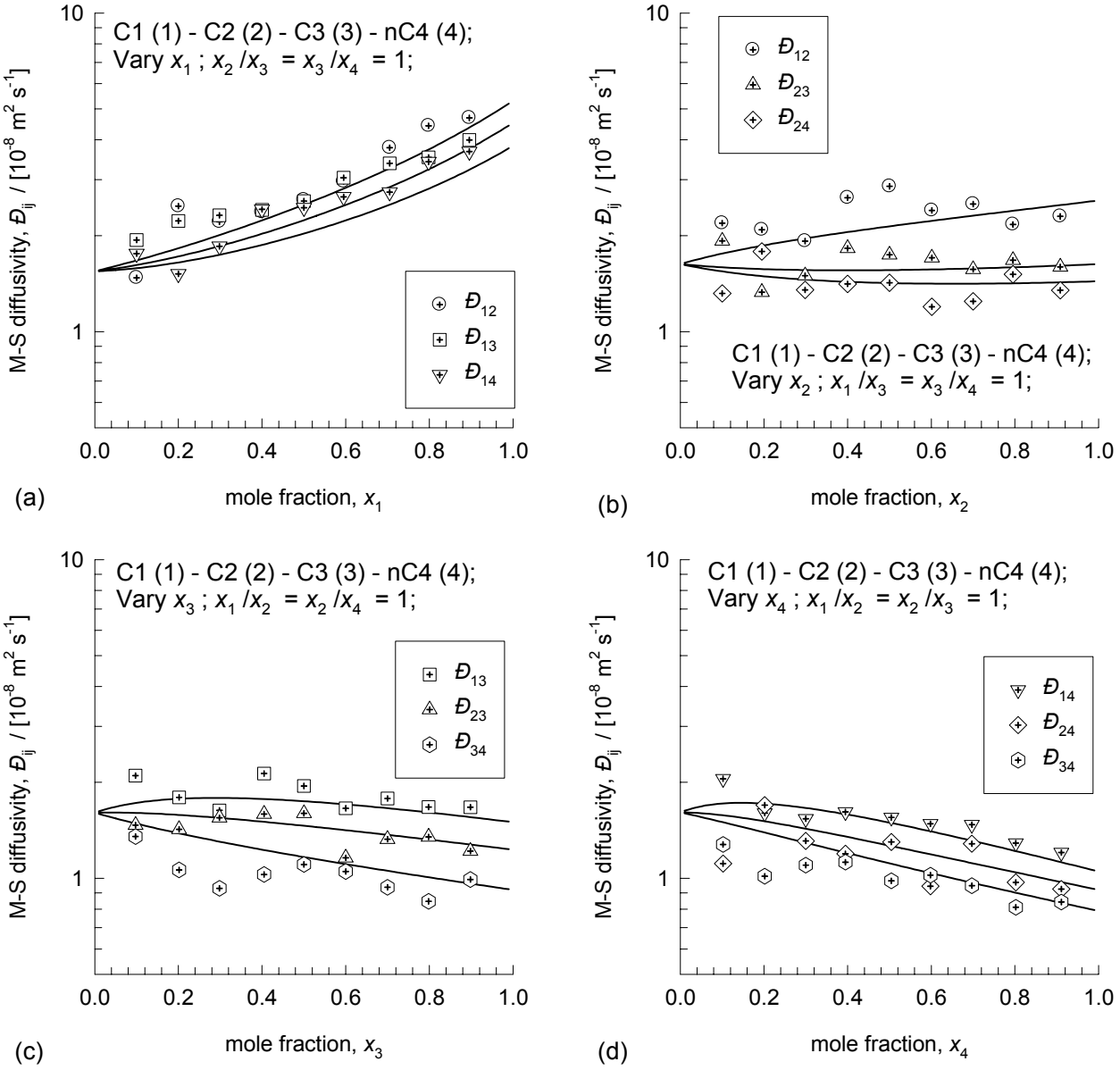

308 K; nC6-nC12, nC6-nC16, and nC12-nC16 binary mixtures

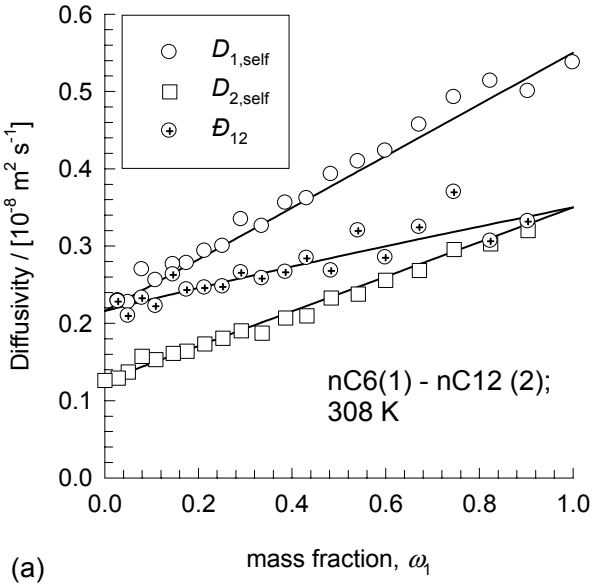

(a)

Molecules in 30 Å box	
nC6	nC12
122	0
112	6
102	11
93	16
85	21
77	26
70	30
63	34
57	38
51	41
45	45
39	48
34	51
29	54
24	57
20	59
15	62
11	64
7	67
4	69
0	71

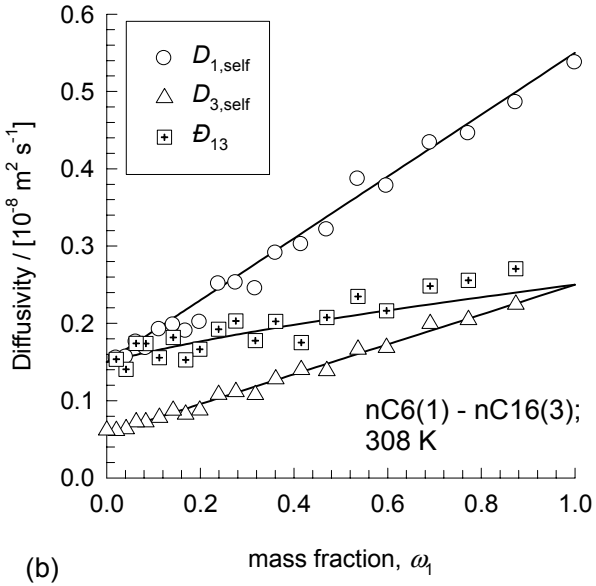

(b)

Molecules in 30 Å box	
nC6	nC16
122	0
109	6
98	11
88	15
78	20
70	23
63	27
56	30
49	33
44	36
38	38
33	40
28	43
24	45
20	46
16	48
12	50
9	51
6	53
3	54
0	55

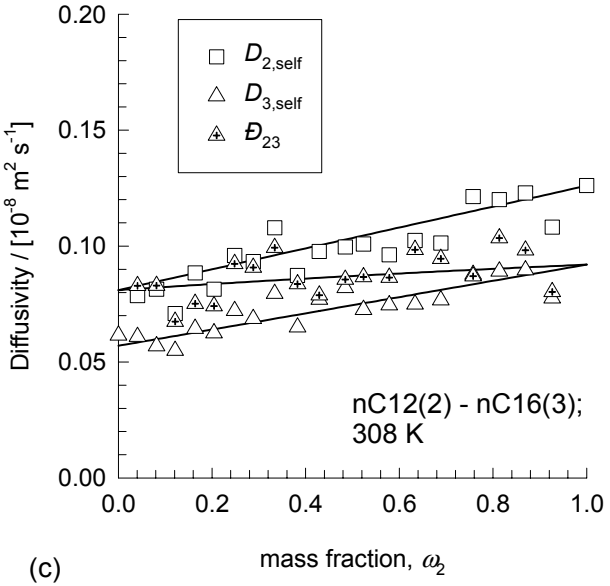

(c)

Molecules in 30 Å box	
nC12	nC16
71	0
67	4
62	7
58	10
54	13
50	17
46	20
42	23
38	26
35	28
31	31
28	34
24	36
21	39
18	41
15	44
12	46
9	49
6	51
3	53
0	55

308 K; nC6-C12-nC16 ternary mixtures

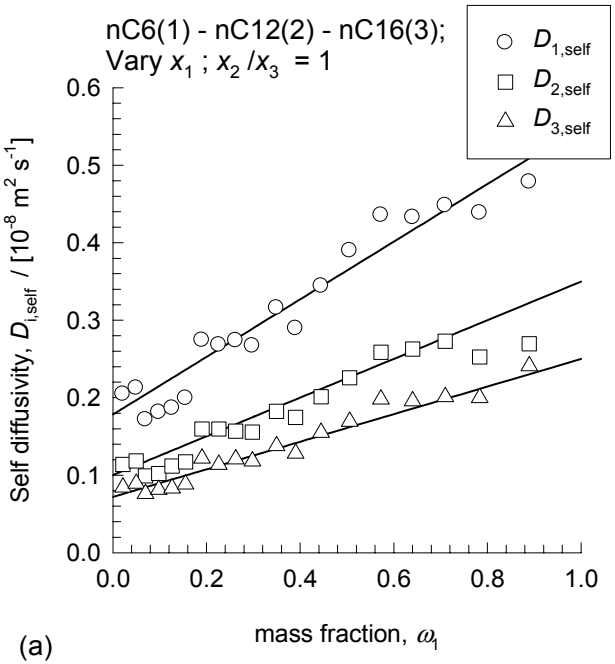

(a)

Molecules in 30 Å box		
nC6	nC12	nC16
3	30	30
7	29	29
10	29	29
14	28	28
18	27	27
22	26	26
26	24	24
31	23	23
36	22	22
41	21	21
47	19	19
53	18	18
59	16	16
66	14	14
74	12	12
82	10	10
90	8	8
100	6	6
111	3	3

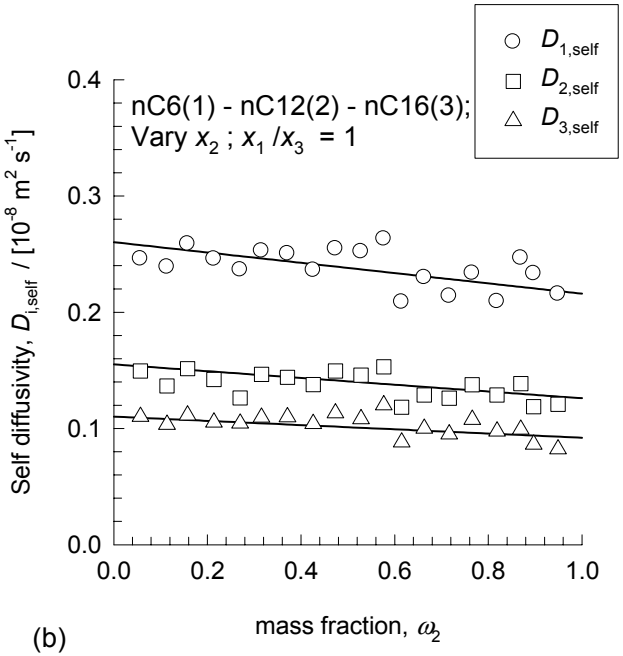

(b)

Molecules in 30 Å box		
nC6	nC12	nC16
36	4	36
34	8	34
32	11	32
30	15	30
28	19	28
26	22	26
24	26	24
22	30	22
20	33	20
18	37	18
16	40	16
15	44	15
13	47	13
11	51	11
9	54	9
7	58	7
5	61	5
4	64	4
2	68	2

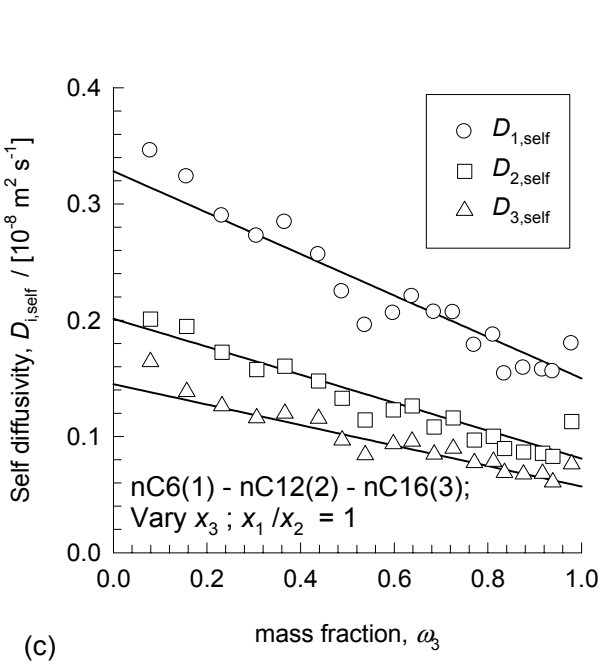

(c)

Molecules in 30 Å box		
nC6	nC12	nC16
41	41	4
38	38	8
35	35	12
32	32	16
29	29	19
26	26	23
24	24	26
22	22	29
19	19	32
17	17	34
15	15	37
13	13	39
11	11	42
9	9	44
8	8	46
6	6	48
4	4	50
3	3	52
1	1	53

308 K; nC6-C12-nC16 ternary mixtures

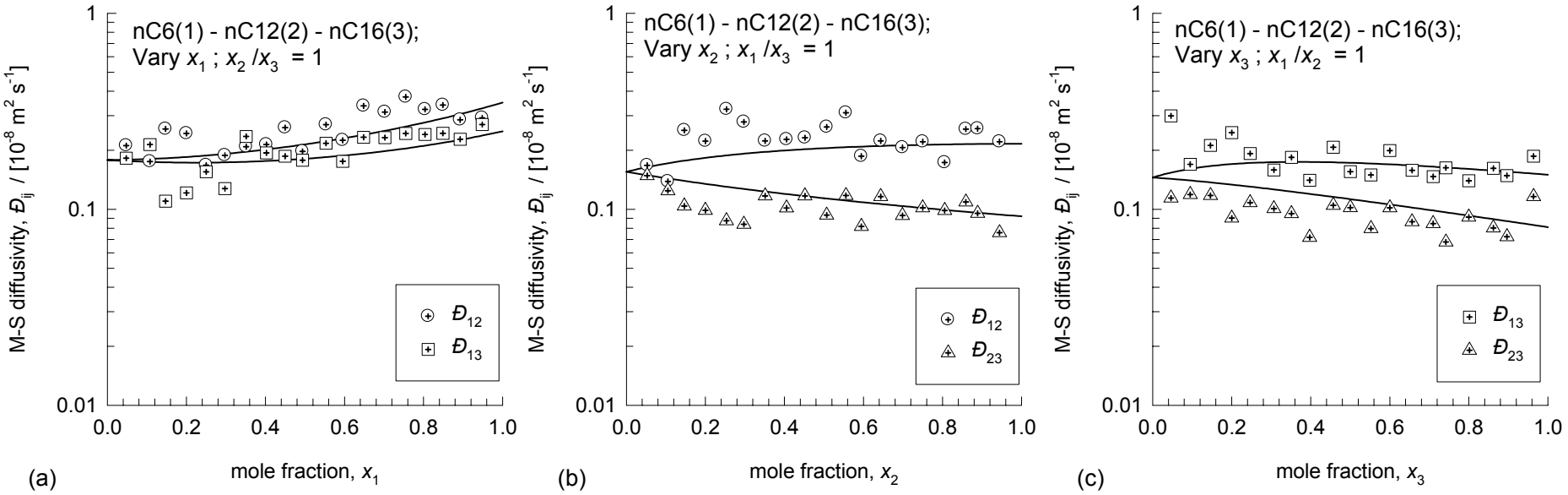

Appendix B

This Appendix gives details of the procedure for calculation of the M-S diffusivities $Đ_{ij}$ from the Onsager coefficients Λ_{ij} determined from MSD data of the MD simulations.

The elements of the *n*-dimensional matrix of Onsager coefficients [Λ] are defined by

$$x_i \mathbf{u}_i = -\frac{1}{RT}\sum_{j=1}^{n} \Lambda_{ij} \nabla \mu_j; \quad i = 1,2,...n \tag{1}$$

If **u** represents the molar average reference velocity

$$\sum_{i=1}^{n} x_i \mathbf{u}_i = \mathbf{u} \tag{2}$$

the M-S equations are written in *n*-1 dimensional matrix form:

$$-\frac{x_i}{RT}\nabla \mu_i = \sum_{j=1}^{n-1} B_{ij} x_j \left(\mathbf{u}_j - \mathbf{u}\right); \quad i = 1,2,..n-1 \tag{3}$$

where we may define an *n*-1 dimensional matrix [*B*]:

$$B_{ii} = \frac{x_i}{Đ_{in}} + \sum_{j=1;\, j\neq i}^{n} \frac{x_j}{Đ_{ij}}; \quad B_{ij} = -x_i\left(\frac{1}{Đ_{ij}} - \frac{1}{Đ_{in}}\right); \quad i,j = 1,2,..n-1 \tag{4}$$

Let us define an *n*-1 dimensional matrix [Δ]

$$[\Delta] = [B]^{-1} \tag{5}$$

The elements Δ_{ij} are related to the Onsager coefficients Λ_{ij} by

$$\Delta_{ij} = (1-x_i)\left(\frac{\Lambda_{ij}}{x_j} - \frac{\Lambda_{in}}{x_n}\right) - x_i \sum_{k=1;\, k\neq i}^{k=n}\left(\frac{\Lambda_{kj}}{x_j} - \frac{\Lambda_{kn}}{x_n}\right); \quad i,j = 1,2,...n-1 \tag{6}$$

where the Onsager coefficients are calculated from the MSD data

$$\Lambda_{ij} = \frac{1}{3N}\int_0^\infty dt \left\langle \sum_{l=1}^{N_i} \mathbf{v}_{i,l}(0) \bullet \sum_{m=1}^{N_j} \mathbf{v}_{j,m}(t) \right\rangle \tag{7}$$

Below we present the detailed derivations of the above set of equations for binary, ternary and quaternary mixtures.

1. Maxwell-Stefan equations for binary mixtures

For binary mixtures the Maxwell-Stefan (M-S) equations:

$$-\frac{1}{RT}\nabla\mu_i = \sum_{j=1;\, j\neq i}^{j=n} \frac{x_j\left(\mathbf{u}_i - \mathbf{u}_j\right)}{Đ_{ij}}; \quad i, j = 1,2,...n \tag{8}$$

reduce to

$$-\frac{1}{RT}\nabla\mu_1 = \frac{x_2\left(\mathbf{u}_1 - \mathbf{u}_2\right)}{Đ_{12}} \tag{9}$$

The molar average reference velocity **u** is

$$\mathbf{u} = x_1\mathbf{u}_1 + x_2\mathbf{u}_2 \tag{10}$$

Substituting eq. (10) into eq. (9) we obtain after simplification with $x_2 = 1 - x_1$

$$-\frac{1}{RT}\nabla\mu_1 = \frac{\left(\mathbf{u}_1 - \mathbf{u}\right)}{Đ_{12}} \tag{11}$$

The set of four Onsager coefficients Λ_{ij}

$$\begin{aligned} x_1\mathbf{u}_1 &= -\frac{1}{RT}\Lambda_{11}\nabla\mu_1 - \frac{1}{RT}\Lambda_{12}\nabla\mu_2 \\ x_2\mathbf{u}_2 &= -\frac{1}{RT}\Lambda_{21}\nabla\mu_1 - \frac{1}{RT}\Lambda_{22}\nabla\mu_2 \end{aligned} \tag{12}$$

are obtained from the MSD data of the MD simulations using

$$\Lambda_{ij} = \frac{1}{3N}\int_0^\infty dt \left\langle \sum_{l=1}^{N_i} \mathbf{v}_{i,l}(0) \bullet \sum_{m=1}^{N_j} \mathbf{v}_{j,m}(t) \right\rangle \tag{13}$$

where $N = N_i + N_j$ is the total number of molecules in the simulation box.

From eq. (12) we can determine the molar average reference velocity **u**

$$\mathbf{u} = x_1\mathbf{u}_1 + x_2\mathbf{u}_2 = -\frac{1}{RT}\Lambda_{11}\nabla\mu_1 - \frac{1}{RT}\Lambda_{12}\nabla\mu_2 - \frac{1}{RT}\Lambda_{21}\nabla\mu_1 - \frac{1}{RT}\Lambda_{22}\nabla\mu_2 \tag{14}$$

Combining eqs (12) and (14) we obtain, after invoking the Gibbs-Duhem equations

$$x_1\nabla\mu_1 + x_2\nabla\mu_2 = 0; \quad -\frac{x_1}{x_2}\nabla\mu_1 = \nabla\mu_2 \tag{15}$$

the following expression

$$\left(\mathbf{u}_1 - \mathbf{u}\right) = -\left(\frac{x_2}{x_1}\Lambda_{11} + \frac{x_1}{x_2}\Lambda_{22} - \Lambda_{12} - \Lambda_{21}\right)\frac{1}{RT}\nabla\mu_1 \tag{16}$$

Comparing with eq. (11) we obtain the following expression for the M-S diffusivity:

$$Đ_{12} = \left[\frac{x_2}{x_1}\Lambda_{11} + \frac{x_1}{x_2}\Lambda_{22} - \Lambda_{12} - \Lambda_{21}\right] \tag{17}$$

2. Maxwell-Stefan equations for ternary mixtures

For ternary mixtures the Maxwell-Stefan (M-S) equations can be cast into the 2-dimensional matrix form:

$$\begin{pmatrix} x_1\left(\mathbf{u}_1 - \mathbf{u}\right) \\ x_2\left(\mathbf{u}_2 - \mathbf{u}\right) \end{pmatrix} = -[B]^{-1}\begin{pmatrix} \frac{x_1}{RT}\nabla\mu_1 \\ \frac{x_2}{RT}\nabla\mu_2 \end{pmatrix} = -[\Delta]\begin{pmatrix} \frac{x_1}{RT}\nabla\mu_1 \\ \frac{x_2}{RT}\nabla\mu_2 \end{pmatrix} \tag{18}$$

which expands to give

$$x_1(\mathbf{u}_1-\mathbf{u})=-\Delta_{11}\frac{x_1}{RT}\nabla\mu_1-\Delta_{12}\frac{x_2}{RT}\nabla\mu_2$$
$$x_2(\mathbf{u}_2-\mathbf{u})=-\Delta_{21}\frac{x_1}{RT}\nabla\mu_1-\Delta_{22}\frac{x_2}{RT}\nabla\mu_2 \tag{19}$$

The set of six Onsager coefficients Λ_{ij} defined by

$$\begin{pmatrix} x_1\mathbf{u}_1 \\ x_2\mathbf{u}_2 \\ x_3\mathbf{u}_3 \end{pmatrix}=-\frac{1}{RT}[\Lambda]\begin{pmatrix} \nabla\mu_1 \\ \nabla\mu_2 \\ \nabla\mu_3 \end{pmatrix} \tag{20}$$

are obtained from the MSD data of the MD simulations using

$$\Lambda_{ij}=\frac{1}{3N}\int_0^\infty dt\left\langle\sum_{l=1}^{N_i}\mathbf{v}_{i,l}(0)\bullet\sum_{m=1}^{N_j}\mathbf{v}_{j,m}(t)\right\rangle \tag{21}$$

Expanding eq. (20)

$$\begin{pmatrix} x_1\mathbf{u}_1 \\ x_2\mathbf{u}_2 \\ x_3\mathbf{u}_3 \end{pmatrix}=-\frac{1}{RT}\begin{pmatrix} \Lambda_{11}\nabla\mu_1+\Lambda_{12}\nabla\mu_2+\Lambda_{13}\nabla\mu_3 \\ \Lambda_{21}\nabla\mu_1+\Lambda_{22}\nabla\mu_2+\Lambda_{23}\nabla\mu_3 \\ \Lambda_{31}\nabla\mu_1+\Lambda_{32}\nabla\mu_2+\Lambda_{33}\nabla\mu_3 \end{pmatrix} \tag{22}$$

We eliminate the chemical potential gradient of component 3 using the Gibbs-Duhem equation

$$x_1\nabla\mu_1+x_2\nabla\mu_2+x_2\nabla\mu_3=0 \tag{23}$$

$$\begin{pmatrix} x_1\mathbf{u}_1 \\ x_2\mathbf{u}_2 \\ x_3\mathbf{u}_3 \end{pmatrix}=-\frac{1}{RT}\begin{pmatrix} \left(\frac{\Lambda_{11}}{x_1}-\frac{\Lambda_{13}}{x_3}\right)x_1\nabla\mu_1+\left(\frac{\Lambda_{12}}{x_2}-\frac{\Lambda_{13}}{x_3}\right)x_2\nabla\mu_2 \\ \left(\frac{\Lambda_{21}}{x_1}-\frac{\Lambda_{23}}{x_3}\right)x_1\nabla\mu_1+\left(\frac{\Lambda_{22}}{x_2}-\frac{\Lambda_{23}}{x_3}\right)x_2\nabla\mu_2 \\ \left(\frac{\Lambda_{31}}{x_1}-\frac{\Lambda_{33}}{x_3}\right)x_1\nabla\mu_1+\left(\frac{\Lambda_{32}}{x_2}-\frac{\Lambda_{33}}{x_3}\right)x_2\nabla\mu_2 \end{pmatrix} \tag{24}$$

The molar average reference velocity **u** is

$$\mathbf{u}RT = (x_1\mathbf{u}_1 + x_2\mathbf{u}_2 + x_3\mathbf{u}_3)RT = -\left(\frac{\Lambda_{11}}{x_1} - \frac{\Lambda_{13}}{x_3}\right)x_1\nabla\mu_1 - \left(\frac{\Lambda_{12}}{x_2} - \frac{\Lambda_{13}}{x_3}\right)x_2\nabla\mu_2$$
$$-\left(\frac{\Lambda_{21}}{x_1} - \frac{\Lambda_{23}}{x_3}\right)x_1\nabla\mu_1 - \left(\frac{\Lambda_{22}}{x_2} - \frac{\Lambda_{23}}{x_3}\right)x_2\nabla\mu_2 - \left(\frac{\Lambda_{31}}{x_1} - \frac{\Lambda_{33}}{x_3}\right)x_1\nabla\mu_1 - \left(\frac{\Lambda_{32}}{x_2} - \frac{\Lambda_{33}}{x_3}\right)x_2\nabla\mu_2 \quad (25)$$

From eqs (24) and (25) we obtain

$$x_1(\mathbf{u}_1 - \mathbf{u})RT = -\left(\frac{\Lambda_{11}}{x_1} - \frac{\Lambda_{13}}{x_3}\right)x_1\nabla\mu_1 - \left(\frac{\Lambda_{12}}{x_2} - \frac{\Lambda_{13}}{x_3}\right)x_2\nabla\mu_2 + x_1\left(\frac{\Lambda_{11}}{x_1} - \frac{\Lambda_{13}}{x_3}\right)x_1\nabla\mu_1 + x_1\left(\frac{\Lambda_{12}}{x_2} - \frac{\Lambda_{13}}{x_3}\right)x_2\nabla\mu_2$$
$$+ x_1\left(\frac{\Lambda_{21}}{x_1} - \frac{\Lambda_{23}}{x_3}\right)x_1\nabla\mu_1 + x_1\left(\frac{\Lambda_{22}}{x_2} - \frac{\Lambda_{23}}{x_3}\right)x_2\nabla\mu_2 + x_1\left(\frac{\Lambda_{31}}{x_1} - \frac{\Lambda_{33}}{x_3}\right)x_1\nabla\mu_1 + x_1\left(\frac{\Lambda_{32}}{x_2} - \frac{\Lambda_{33}}{x_3}\right)x_2\nabla\mu_2 \quad (26)$$

$$x_2(\mathbf{u}_2 - \mathbf{u})RT = -\left(\frac{\Lambda_{21}}{x_1} - \frac{\Lambda_{23}}{x_3}\right)x_1\nabla\mu_1 - \left(\frac{\Lambda_{22}}{x_2} - \frac{\Lambda_{23}}{x_3}\right)x_2\nabla\mu_2 + x_2\left(\frac{\Lambda_{11}}{x_1} - \frac{\Lambda_{13}}{x_3}\right)x_1\nabla\mu_1 + x_2\left(\frac{\Lambda_{12}}{x_2} - \frac{\Lambda_{13}}{x_3}\right)x_2\nabla\mu_2$$
$$+ x_2\left(\frac{\Lambda_{21}}{x_1} - \frac{\Lambda_{23}}{x_3}\right)x_1\nabla\mu_1 + x_2\left(\frac{\Lambda_{22}}{x_2} - \frac{\Lambda_{23}}{x_3}\right)x_2\nabla\mu_2 + x_2\left(\frac{\Lambda_{31}}{x_1} - \frac{\Lambda_{33}}{x_3}\right)x_1\nabla\mu_1 + x_2\left(\frac{\Lambda_{32}}{x_2} - \frac{\Lambda_{33}}{x_3}\right)x_2\nabla\mu_2 \quad (27)$$

Comparing term by term with eq. (19) we obtain the following relations relating the Δ_{ij} to the Λ_{ij}

$$\Delta_{11} = (1-x_1)\left(\frac{\Lambda_{11}}{x_1} - \frac{\Lambda_{13}}{x_3}\right) - x_1\left(\frac{\Lambda_{21}}{x_1} - \frac{\Lambda_{23}}{x_3} + \frac{\Lambda_{31}}{x_1} - \frac{\Lambda_{33}}{x_3}\right) \quad (28)$$

$$\Delta_{12} = (1-x_1)\left(\frac{\Lambda_{12}}{x_2} - \frac{\Lambda_{13}}{x_3}\right) - x_1\left(\frac{\Lambda_{22}}{x_2} - \frac{\Lambda_{23}}{x_3} + \frac{\Lambda_{32}}{x_2} - \frac{\Lambda_{33}}{x_3}\right) \quad (29)$$

$$\Delta_{21} = (1-x_2)\left(\frac{\Lambda_{21}}{x_1} - \frac{\Lambda_{23}}{x_3}\right) - x_2\left(\frac{\Lambda_{11}}{x_1} - \frac{\Lambda_{13}}{x_3} + \frac{\Lambda_{31}}{x_1} - \frac{\Lambda_{33}}{x_3}\right) \quad (30)$$

$$\Delta_{22} = (1-x_2)\left(\frac{\Lambda_{22}}{x_2} - \frac{\Lambda_{23}}{x_3}\right) - x_2\left(\frac{\Lambda_{12}}{x_2} - \frac{\Lambda_{13}}{x_3} + \frac{\Lambda_{32}}{x_2} - \frac{\Lambda_{33}}{x_3}\right) \quad (31)$$

The matrix [Δ] can be inverted to obtain the four elements of the matrix [B]

$$[B] = [\Delta]^{-1} \quad (32)$$

Explicity, the four elements of the matrix [B] are

$$B_{11} = \frac{x_1}{Đ_{13}} + \frac{x_2}{Đ_{12}} + \frac{x_3}{Đ_{13}} \tag{33}$$

$$B_{12} = -x_1\left(\frac{1}{Đ_{12}} - \frac{1}{Đ_{13}}\right) \tag{34}$$

$$B_{21} = -x_2\left(\frac{1}{Đ_{12}} - \frac{1}{Đ_{23}}\right) \tag{35}$$

$$B_{22} = \frac{x_2}{Đ_{23}} + \frac{x_1}{Đ_{12}} + \frac{x_3}{Đ_{23}} \tag{36}$$

The three M-S diffusivities can be calculated as follows

$$Đ_{13} = \frac{1}{B_{11} + \dfrac{x_2 B_{12}}{x_1}} \tag{37}$$

$$Đ_{12} = \frac{1}{B_{11} - \dfrac{(x_1 + x_3)}{x_1} B_{12}} \tag{38}$$

$$Đ_{23} = \frac{1}{B_{22} + \dfrac{x_1 B_{21}}{x_2}} \tag{39}$$

3. Maxwell-Stefan equations for quaternary mixtures

For quaternary mixtures the Onsager diffusion equations are

$$\begin{pmatrix} x_1\mathbf{u}_1 \\ x_2\mathbf{u}_2 \\ x_3\mathbf{u}_3 \\ x_4\mathbf{u}_4 \end{pmatrix} = -\frac{1}{RT}\begin{pmatrix} \Lambda_{11}\nabla\mu_1 + \Lambda_{12}\nabla\mu_2 + \Lambda_{13}\nabla\mu_3 + \Lambda_{14}\nabla\mu_4 \\ \Lambda_{21}\nabla\mu_1 + \Lambda_{22}\nabla\mu_2 + \Lambda_{23}\nabla\mu_3 + \Lambda_{24}\nabla\mu_4 \\ \Lambda_{31}\nabla\mu_1 + \Lambda_{32}\nabla\mu_2 + \Lambda_{33}\nabla\mu_3 + \Lambda_{34}\nabla\mu_4 \\ \Lambda_{41}\nabla\mu_1 + \Lambda_{42}\nabla\mu_2 + \Lambda_{43}\nabla\mu_3 + \Lambda_{44}\nabla\mu_4 \end{pmatrix} \tag{40}$$

The chemical potential driving force for the fourth species can be eliminated using the Gibbs-Duhem equation

$$x_1\nabla\mu_1 + x_2\nabla\mu_2 + x_3\nabla\mu_3 + x_4\nabla\mu_4 = 0 \tag{41}$$

to obtain

$$\begin{pmatrix} x_1\mathbf{u}_1 \\ x_2\mathbf{u}_2 \\ x_3\mathbf{u}_3 \\ x_4\mathbf{u}_4 \end{pmatrix} = -\frac{1}{RT}\begin{pmatrix} \left(\frac{\Lambda_{11}}{x_1}-\frac{\Lambda_{14}}{x_4}\right)x_1\nabla\mu_1 + \left(\frac{\Lambda_{12}}{x_2}-\frac{\Lambda_{14}}{x_4}\right)x_2\nabla\mu_2 + \left(\frac{\Lambda_{13}}{x_3}-\frac{\Lambda_{14}}{x_4}\right)x_3\nabla\mu_3 \\ \left(\frac{\Lambda_{21}}{x_1}-\frac{\Lambda_{24}}{x_4}\right)x_1\nabla\mu_1 + \left(\frac{\Lambda_{22}}{x_2}-\frac{\Lambda_{24}}{x_4}\right)x_2\nabla\mu_2 + \left(\frac{\Lambda_{23}}{x_3}-\frac{\Lambda_{24}}{x_4}\right)x_3\nabla\mu_3 \\ \left(\frac{\Lambda_{31}}{x_1}-\frac{\Lambda_{34}}{x_4}\right)x_1\nabla\mu_1 + \left(\frac{\Lambda_{32}}{x_2}-\frac{\Lambda_{34}}{x_4}\right)x_2\nabla\mu_2 + \left(\frac{\Lambda_{33}}{x_3}-\frac{\Lambda_{34}}{x_4}\right)x_3\nabla\mu_3 \\ \left(\frac{\Lambda_{41}}{x_1}-\frac{\Lambda_{44}}{x_4}\right)x_1\nabla\mu_1 + \left(\frac{\Lambda_{42}}{x_2}-\frac{\Lambda_{44}}{x_4}\right)x_2\nabla\mu_2 + \left(\frac{\Lambda_{43}}{x_3}-\frac{\Lambda_{44}}{x_4}\right)x_3\nabla\mu_3 \end{pmatrix} \tag{42}$$

The molar average reference velocity **u** is

$$\begin{aligned} -\mathbf{u}RT = -(x_1\mathbf{u}_1 + x_2\mathbf{u}_2 + x_3\mathbf{u}_3 + x_4\mathbf{u}_4)RT = \\ \left(\frac{\Lambda_{11}}{x_1}-\frac{\Lambda_{14}}{x_4}\right)x_1\nabla\mu_1 + \left(\frac{\Lambda_{12}}{x_2}-\frac{\Lambda_{14}}{x_4}\right)x_2\nabla\mu_2 + \left(\frac{\Lambda_{13}}{x_3}-\frac{\Lambda_{14}}{x_4}\right)x_3\nabla\mu_3 + \\ \left(\frac{\Lambda_{21}}{x_1}-\frac{\Lambda_{24}}{x_4}\right)x_1\nabla\mu_1 + \left(\frac{\Lambda_{22}}{x_2}-\frac{\Lambda_{24}}{x_4}\right)x_2\nabla\mu_2 + \left(\frac{\Lambda_{23}}{x_3}-\frac{\Lambda_{24}}{x_4}\right)x_3\nabla\mu_3 + \\ \left(\frac{\Lambda_{31}}{x_1}-\frac{\Lambda_{34}}{x_4}\right)x_1\nabla\mu_1 + \left(\frac{\Lambda_{32}}{x_2}-\frac{\Lambda_{34}}{x_4}\right)x_2\nabla\mu_2 + \left(\frac{\Lambda_{33}}{x_3}-\frac{\Lambda_{34}}{x_4}\right)x_3\nabla\mu_3 + \\ \left(\frac{\Lambda_{41}}{x_1}-\frac{\Lambda_{44}}{x_4}\right)x_1\nabla\mu_1 + \left(\frac{\Lambda_{42}}{x_2}-\frac{\Lambda_{44}}{x_4}\right)x_2\nabla\mu_2 + \left(\frac{\Lambda_{43}}{x_3}-\frac{\Lambda_{44}}{x_4}\right)x_3\nabla\mu_3 \end{aligned} \tag{43}$$

Combining eqs (42) and (43) we obtain

$$
\begin{aligned}
&x_1(\mathbf{u}_1-\mathbf{u})RT = \\
&-\left(\frac{\Lambda_{11}}{x_1}-\frac{\Lambda_{14}}{x_4}\right)x_1\nabla\mu_1-\left(\frac{\Lambda_{12}}{x_2}-\frac{\Lambda_{14}}{x_4}\right)x_2\nabla\mu_2-\left(\frac{\Lambda_{13}}{x_3}-\frac{\Lambda_{14}}{x_4}\right)x_3\nabla\mu_3 \\
&x_1\left(\frac{\Lambda_{11}}{x_1}-\frac{\Lambda_{14}}{x_4}\right)x_1\nabla\mu_1+x_1\left(\frac{\Lambda_{12}}{x_2}-\frac{\Lambda_{14}}{x_4}\right)x_2\nabla\mu_2+x_1\left(\frac{\Lambda_{13}}{x_3}-\frac{\Lambda_{14}}{x_4}\right)x_3\nabla\mu_3+ \\
&x_1\left(\frac{\Lambda_{21}}{x_1}-\frac{\Lambda_{24}}{x_4}\right)x_1\nabla\mu_1+x_1\left(\frac{\Lambda_{22}}{x_2}-\frac{\Lambda_{24}}{x_4}\right)x_2\nabla\mu_2+x_1\left(\frac{\Lambda_{23}}{x_3}-\frac{\Lambda_{24}}{x_4}\right)x_3\nabla\mu_3+ \\
&x_1\left(\frac{\Lambda_{31}}{x_1}-\frac{\Lambda_{34}}{x_4}\right)x_1\nabla\mu_1+x_1\left(\frac{\Lambda_{32}}{x_2}-\frac{\Lambda_{34}}{x_4}\right)x_2\nabla\mu_2+x_1\left(\frac{\Lambda_{33}}{x_3}-\frac{\Lambda_{34}}{x_4}\right)x_3\nabla\mu_3+ \\
&x_1\left(\frac{\Lambda_{41}}{x_1}-\frac{\Lambda_{44}}{x_4}\right)x_1\nabla\mu_1+x_1\left(\frac{\Lambda_{42}}{x_2}-\frac{\Lambda_{44}}{x_4}\right)x_2\nabla\mu_2+x_1\left(\frac{\Lambda_{43}}{x_3}-\frac{\Lambda_{44}}{x_4}\right)x_3\nabla\mu_3
\end{aligned}
\tag{44}
$$

$$
\begin{aligned}
&x_2(\mathbf{u}_2-\mathbf{u})RT = \\
&-\left(\frac{\Lambda_{21}}{x_1}-\frac{\Lambda_{24}}{x_4}\right)x_1\nabla\mu_1-\left(\frac{\Lambda_{22}}{x_2}-\frac{\Lambda_{24}}{x_4}\right)x_2\nabla\mu_2-\left(\frac{\Lambda_{23}}{x_3}-\frac{\Lambda_{24}}{x_4}\right)x_3\nabla\mu_3 \\
&x_2\left(\frac{\Lambda_{11}}{x_1}-\frac{\Lambda_{14}}{x_4}\right)x_1\nabla\mu_1+x_2\left(\frac{\Lambda_{12}}{x_2}-\frac{\Lambda_{14}}{x_4}\right)x_2\nabla\mu_2+x_2\left(\frac{\Lambda_{13}}{x_3}-\frac{\Lambda_{14}}{x_4}\right)x_3\nabla\mu_3+ \\
&x_2\left(\frac{\Lambda_{21}}{x_1}-\frac{\Lambda_{24}}{x_4}\right)x_1\nabla\mu_1+x_2\left(\frac{\Lambda_{22}}{x_2}-\frac{\Lambda_{24}}{x_4}\right)x_2\nabla\mu_2+x_2\left(\frac{\Lambda_{23}}{x_3}-\frac{\Lambda_{24}}{x_4}\right)x_3\nabla\mu_3+ \\
&x_2\left(\frac{\Lambda_{31}}{x_1}-\frac{\Lambda_{34}}{x_4}\right)x_1\nabla\mu_1+x_2\left(\frac{\Lambda_{32}}{x_2}-\frac{\Lambda_{34}}{x_4}\right)x_2\nabla\mu_2+x_2\left(\frac{\Lambda_{33}}{x_3}-\frac{\Lambda_{34}}{x_4}\right)x_3\nabla\mu_3+ \\
&x_2\left(\frac{\Lambda_{41}}{x_1}-\frac{\Lambda_{44}}{x_4}\right)x_1\nabla\mu_1+x_2\left(\frac{\Lambda_{42}}{x_2}-\frac{\Lambda_{44}}{x_4}\right)x_2\nabla\mu_2+x_2\left(\frac{\Lambda_{43}}{x_3}-\frac{\Lambda_{44}}{x_4}\right)x_3\nabla\mu_3
\end{aligned}
\tag{45}
$$

$$
\begin{aligned}
&x_3(\mathbf{u}_3-\mathbf{u})RT = \\
&-\left(\frac{\Lambda_{31}}{x_1}-\frac{\Lambda_{34}}{x_4}\right)x_1\nabla\mu_1-\left(\frac{\Lambda_{32}}{x_2}-\frac{\Lambda_{34}}{x_4}\right)x_2\nabla\mu_2-\left(\frac{\Lambda_{33}}{x_3}-\frac{\Lambda_{34}}{x_4}\right)x_3\nabla\mu_3 \\
&x_3\left(\frac{\Lambda_{11}}{x_1}-\frac{\Lambda_{14}}{x_4}\right)x_1\nabla\mu_1+x_3\left(\frac{\Lambda_{12}}{x_2}-\frac{\Lambda_{14}}{x_4}\right)x_2\nabla\mu_2+x_3\left(\frac{\Lambda_{13}}{x_3}-\frac{\Lambda_{14}}{x_4}\right)x_3\nabla\mu_3+ \\
&x_3\left(\frac{\Lambda_{21}}{x_1}-\frac{\Lambda_{24}}{x_4}\right)x_1\nabla\mu_1+x_3\left(\frac{\Lambda_{22}}{x_2}-\frac{\Lambda_{24}}{x_4}\right)x_2\nabla\mu_2+x_3\left(\frac{\Lambda_{23}}{x_3}-\frac{\Lambda_{24}}{x_4}\right)x_3\nabla\mu_3+ \\
&x_3\left(\frac{\Lambda_{31}}{x_1}-\frac{\Lambda_{34}}{x_4}\right)x_1\nabla\mu_1+x_3\left(\frac{\Lambda_{32}}{x_2}-\frac{\Lambda_{34}}{x_4}\right)x_2\nabla\mu_2+x_3\left(\frac{\Lambda_{33}}{x_3}-\frac{\Lambda_{34}}{x_4}\right)x_3\nabla\mu_3+ \\
&x_3\left(\frac{\Lambda_{41}}{x_1}-\frac{\Lambda_{44}}{x_4}\right)x_1\nabla\mu_1+x_3\left(\frac{\Lambda_{42}}{x_2}-\frac{\Lambda_{44}}{x_4}\right)x_2\nabla\mu_2+x_3\left(\frac{\Lambda_{43}}{x_3}-\frac{\Lambda_{44}}{x_4}\right)x_3\nabla\mu_3
\end{aligned}
\tag{46}
$$

The M-S equations can be written in 3-dimensional matrix form as

$$\begin{pmatrix} x_1(\mathbf{u}_1-\mathbf{u}) \\ x_2(\mathbf{u}_2-\mathbf{u}) \\ x_3(\mathbf{u}_3-\mathbf{u}) \end{pmatrix} = -[B]^{-1}\frac{1}{RT}\begin{pmatrix} x_1\nabla\mu_1 \\ x_2\nabla\mu_2 \\ x_3\nabla\mu_3 \end{pmatrix} = -[\Delta]\frac{1}{RT}\begin{pmatrix} x_1\nabla\mu_1 \\ x_2\nabla\mu_2 \\ x_3\nabla\mu_3 \end{pmatrix} \tag{47}$$

Comparing eq. (47) with eqs (44), (45), and (46), term by term, we obtain the following expressions relating the Δ_{ij} to the Λ_{ij}

$$\Delta_{12} = (1-x_1)\left(\frac{\Lambda_{12}}{x_2}-\frac{\Lambda_{14}}{x_4}\right) - x_1\left(\frac{\Lambda_{22}}{x_2}-\frac{\Lambda_{24}}{x_4}+\frac{\Lambda_{32}}{x_2}-\frac{\Lambda_{34}}{x_4}+\frac{\Lambda_{42}}{x_2}-\frac{\Lambda_{44}}{x_4}\right) \tag{48}$$

$$\Delta_{13} = (1-x_1)\left(\frac{\Lambda_{13}}{x_3}-\frac{\Lambda_{14}}{x_4}\right) - x_1\left(\frac{\Lambda_{23}}{x_3}-\frac{\Lambda_{24}}{x_4}+\frac{\Lambda_{33}}{x_3}-\frac{\Lambda_{34}}{x_4}+\frac{\Lambda_{43}}{x_3}-\frac{\Lambda_{44}}{x_4}\right) \tag{49}$$

$$\Delta_{21} = (1-x_2)\left(\frac{\Lambda_{21}}{x_1}-\frac{\Lambda_{24}}{x_4}\right) - x_2\left(\frac{\Lambda_{11}}{x_1}-\frac{\Lambda_{14}}{x_4}+\frac{\Lambda_{31}}{x_1}-\frac{\Lambda_{34}}{x_4}+\frac{\Lambda_{41}}{x_1}-\frac{\Lambda_{44}}{x_4}\right) \tag{50}$$

$$\Delta_{22} = (1-x_2)\left(\frac{\Lambda_{22}}{x_2}-\frac{\Lambda_{24}}{x_4}\right) - x_2\left(\frac{\Lambda_{12}}{x_2}-\frac{\Lambda_{14}}{x_4}+\frac{\Lambda_{32}}{x_2}-\frac{\Lambda_{34}}{x_4}+\frac{\Lambda_{42}}{x_2}-\frac{\Lambda_{44}}{x_4}\right) \tag{51}$$

$$\Delta_{23} = (1-x_2)\left(\frac{\Lambda_{23}}{x_3}-\frac{\Lambda_{24}}{x_4}\right) - x_2\left(\frac{\Lambda_{13}}{x_3}-\frac{\Lambda_{14}}{x_4}+\frac{\Lambda_{33}}{x_3}-\frac{\Lambda_{34}}{x_4}+\frac{\Lambda_{43}}{x_3}-\frac{\Lambda_{44}}{x_4}\right) \tag{52}$$

$$\Delta_{31} = (1-x_3)\left(\frac{\Lambda_{31}}{x_1}-\frac{\Lambda_{34}}{x_4}\right) - x_3\left(\frac{\Lambda_{11}}{x_1}-\frac{\Lambda_{14}}{x_4}+\frac{\Lambda_{21}}{x_1}-\frac{\Lambda_{24}}{x_4}+\frac{\Lambda_{41}}{x_1}-\frac{\Lambda_{44}}{x_4}\right) \tag{53}$$

$$\Delta_{32} = (1-x_3)\left(\frac{\Lambda_{32}}{x_2}-\frac{\Lambda_{34}}{x_4}\right) - x_3\left(\frac{\Lambda_{12}}{x_2}-\frac{\Lambda_{14}}{x_4}+\frac{\Lambda_{22}}{x_2}-\frac{\Lambda_{24}}{x_4}+\frac{\Lambda_{42}}{x_2}-\frac{\Lambda_{44}}{x_4}\right) \tag{54}$$

$$\Delta_{33} = (1-x_3)\left(\frac{\Lambda_{33}}{x_3}-\frac{\Lambda_{34}}{x_4}\right) - x_3\left(\frac{\Lambda_{13}}{x_3}-\frac{\Lambda_{14}}{x_4}+\frac{\Lambda_{23}}{x_3}-\frac{\Lambda_{24}}{x_4}+\frac{\Lambda_{43}}{x_3}-\frac{\Lambda_{44}}{x_4}\right) \tag{55}$$

The matrix [Δ] can be inverted to obtain the nine elements of the matrix [*B*]

$$[B]=[\Delta]^{-1} \tag{56}$$

Explicity, the nine elements of the matrix [B] are

$$B_{11}=\frac{x_1}{Đ_{14}}+\frac{x_2}{Đ_{12}}+\frac{x_3}{Đ_{13}}+\frac{x_4}{Đ_{14}} \tag{57}$$

$$B_{11}=\frac{x_1+x_4}{Đ_{14}}+\frac{x_2}{Đ_{12}}+\frac{x_3}{Đ_{13}} \tag{58}$$

$$B_{12}=-x_1\left(\frac{1}{Đ_{12}}-\frac{1}{Đ_{14}}\right) \tag{59}$$

$$B_{13}=-x_1\left(\frac{1}{Đ_{13}}-\frac{1}{Đ_{14}}\right) \tag{60}$$

$$B_{21}=-x_2\left(\frac{1}{Đ_{12}}-\frac{1}{Đ_{24}}\right) \tag{61}$$

$$B_{22}=\frac{x_2+x_4}{Đ_{24}}+\frac{x_1}{Đ_{12}}+\frac{x_3}{Đ_{23}} \tag{62}$$

$$B_{23}=-x_2\left(\frac{1}{Đ_{23}}-\frac{1}{Đ_{24}}\right) \tag{63}$$

$$B_{31}=-x_3\left(\frac{1}{Đ_{13}}-\frac{1}{Đ_{34}}\right) \tag{64}$$

$$B_{32}=-x_3\left(\frac{1}{Đ_{23}}-\frac{1}{Đ_{34}}\right) \tag{65}$$

$$B_{33}=\frac{x_3+x_4}{Đ_{34}}+\frac{x_1}{Đ_{13}}+\frac{x_2}{Đ_{23}} \tag{66}$$

The six M-S pair diffusivities can be calculated as follows

$$Đ_{14} = \frac{1}{B_{11} + \frac{x_2}{x_1} B_{12} + \frac{x_3}{x_1} B_{13}} \tag{67}$$

$$Đ_{24} = \frac{1}{B_{22} + \frac{x_1}{x_2} B_{21} + \frac{x_3}{x_2} B_{23}} \tag{68}$$

$$Đ_{34} = \frac{1}{B_{33} + \frac{x_1}{x_3} B_{31} + \frac{x_2}{x_3} B_{32}} \tag{69}$$

$$Đ_{12} = \frac{1}{\frac{1}{Đ_{24}} - \frac{B_{21}}{x_2}} \tag{70}$$

$$Đ_{13} = \frac{1}{\frac{1}{Đ_{14}} - \frac{B_{13}}{x_1}} \tag{71}$$

$$Đ_{23} = \frac{1}{\frac{1}{Đ_{24}} - \frac{B_{23}}{x_2}} \tag{72}$$